SULFATED COMPOUNDS IN THE ZYMOGEN GRANULES

OF THE GUINEA PIG PANCREAS

HUBERT A. REGGIO and GEORGE E. PALADE

From the Section of Cell Biology, Yale University Medical School, New Haven, Connecticut
06510. Dr. Reggio's present address is the Institut de Chimie Biologique, Faculté des Sciences,
Université de Provence, 13331 Marseille, France.

ABSTRACT

Sulfate incorporation into the guinea pig pancreas was investigated by light (LM) and electron microscope (EM) autoradiography using a system of minilobules incubated in vitro for 60 min in Krebs-Ringer bicarbonate medium (KRB) containing $^{35}SO_4^{2-}$. In acinar cells, examined by EM autoradiography, the label was found concentrated over Golgi elements (including condensing vacuoles) and zymogen granules.

$^{35}SO_4^{2-}$ was also incorporated by the epithelial cells of the entire pancreatic duct system, the incorporation being surprisingly high in the epithelium of the major ducts. In all ductal epithelia, autoradiographic grains appeared over the Golgi complex and the plasmalemma.

Since a contribution of the duct epithelium to the sulfated compounds found in the discharged secretion could not be ruled out, a purified zymogen granule fraction was used as a source material for the isolation of sulfated compounds of acinar origin. The presence of ^{35}S-radioactivity in the zymogen granules and condensing vacuoles of this fraction was ascertained by autoradiography (of sectioned pellets). From a lysate of this zymogen granule fraction, a soluble sulfated compound of low isoelectric point and high molecular weight was isolated by gel filtration under conditions that allowed its satisfactory separation from the bulk of the secretory proteins.

KEY WORDS   sulfated macromolecules ·
secretion products · pancreatic
secretion granules · $^{35}SO_4^{2-}$ incorporation ·
Golgi complex · autoradiography

Macromolecular sulfated compounds have been detected in the secretory granules of a variety of cells by either autoradiography or biochemical analyses of cell fractions. In some cases, the sulfated compounds were recognized as major secretory products of the cells studied, e.g., heparin in mast cells (26), mucopolysaccharides in goblet cells (27, 29), and sulfated peptidoglycans in chondrocytes (18). But in other cases, such compounds were found to be minority components of still undefined function apparently packaged and stored together with the main products of the cells within the same secretion granules. For instance, chondroitin sulfate A was isolated from leukocyte and platelet granules (33), and small quantities of heparan sulfate, heparin, and chondroitin sulfate were detected in prolactin granules isolated from rat pituitaries (16).

In vivo incorporation of $^{35}SO_4^{2-}$ into unidentified macromolecular components was demonstrated by autoradiography in the Golgi complex of a wide variety of cell types (50). Sulfated compounds were also detected in Golgi fractions isolated from liver homogenates after in vivo labeling (23). By contrast, evidence for the in vitro incorporation of $^{35}SO_4^{2-}$ into glycoproteins and glycolipids is still limited to Golgi fractions isolated from kidney (15).

In the case of the pancreatic exocrine cell, evidence concerning the presence of sulfated macromolecular compounds in secretory granules was obtained by both autoradiography and radiochemical assays, but in different species and under different experimental conditions. Berg and Young (8) demonstrated by autoradiography the presence of ^{35}S in the Golgi complex, secretion granules, and discharged secretion in the mouse pancreas after incorporation of $^{35}SO_4^{2-}$ in vivo, while Tartakoff et al. (44) showed that guinea pig pancreatic lobules incorporated $^{35}SO_4^{2-}$ into high molecular weight compounds of low pI (~3.4) which could be detected by radiochemical assays in discharged secretion as well as in the content extracted from isolated zymogen granules. In conjunction with the latter finding, it was postulated that these sulfated polyanions play a role in the concentration of secretory products within Golgi condensing vacuoles, presumably by ionic interactions with the predominantly cationic secretory proteins of this species. Such interactions could lead to aggregate formation and reduction in osmotic activity within compartments containing the sulfated polyanions (44). Before putting this hypothesis to test, we felt that additional data were needed to define in sufficient detail the incorporation of $^{35}SO_4^{2-}$ in guinea pig lobules. In this paper we report our results on: (a) the kinetics of $^{35}SO_4^{2-}$ incorporation; (b) the identification by autoradiography of multiple sites of synthesis of sulfated compounds within the pancreatic tissue; and (c) the isolation and partial characterization of sulfated polyanions from zymogen granules.

MATERIALS AND METHODS

(a) Animals

The guinea pigs came from the Yale University colony, weighed 300-350 g, and were fasted (with water ad libitum) for 24 h before each experiment.

(b) Tissue Preparation

Two different in vitro systems were used. The first was the lobule preparation described by Scheele and Palade (42) which consists of small clusters of lobules dissected from a pancreas distended by injecting Krebs-Ringer bicarbonate solution (KRB)[1] or incubation medium (see below) into its loose connective tissue. SO_4^{2-}-free and/or leucine-free incubation medium was used when lobules were prepared for labeling experiments. The second was the minilobule preparation recently introduced by Amsterdam et al. (3); it is obtained by collagenase digestion (in full KRB) and shearing of the glandular tissue, and it consists of lobules or clusters of acini four to five times smaller than those of the first preparation. After shearing, the minilobules were collected by centrifugation (150 g × 1 min) and washed three times by resuspension-recentrifugation in KRB, or in SO_4^{2-}-free and/or leucine-free incubation media (when prepared for labeling experiments). During washing, duct and blood vessel fragments were carefully removed (with fine forceps) from the suspension.

Ducts were isolated by dissection (under a stereo microscope) from glands distended by injected KRB or incubation medium (as above), and were incubated directly or after collagenase treatment. In the latter case, the preparation was vigorously pipetted three times through a polyethylene pipet (tip diameter ≈ 1 mm) and three times through a siliconized glass pipette (tip diameter ≈ 0.5 mm). After the last step, duct fragments which appeared well preserved were picked up with fine forceps, washed as done in the case of minilobules, and incubated separately. Under the light microscope (LM) such fargments appeared to be almost completely freed of surrounding acini.

(c) Incubation Media

All incubations were carried out in KRB equilibrated to pH 7.3 with 95% O_2-5% CO_2 and supplemented with glucose (11 mM) and a complete set of amino acids (14). When radioactive leucine was added to the medium, nonradioactive leucine was omitted, and when $^{35}SO_4^{2-}$ was used, the $MgSO_4$ in KRB was replaced with an equimolar amount of $MgCl_2$. Minilobules were always incubated in KRB containing 10 mg/ml bovine plasma albumin (BPA) and 0.1 mg/ml soybean trypsin inhibitor (STI). All media were filtered

---

[1] *Abbreviations used in this paper*: BPA: bovine plasma albumin; EDTA: ethylenediaminetetraacetate; KRB: Krebs-Ringer bicarbonate solution; EM: electron microscope; HD: half distance; LM: light microscope; PPO: 2,5-diphenyloxazole; POPOP: 1,4-bis[2-(5-phenyloxazolyl)]benzene; RER: rough endoplasmic reticulum; SDS: sodium dodecyl sulfate; STI: soybean trypsin inhibitor; TCA: trichloroacetic acid; Tris: tris(hydroxymethyl)aminomethane.

through a 0.45-μm filter (Millipore Corp., Bedbord, Mass.) and all glassware was siliconized before use.

(d) Labeling Conditions

To establish optimal conditions for $^{35}SO_4^{2-}$ incorporation, lobules were incubated for different time periods in 10 ml of SO_4^{2-}-free KRB in the presence of 100 μCi/ml of $^{35}SO_4^{2-}$. The incubated lobules were homogenized and the trichloroacetic acid (TCA)-precipitable radioactivity of the homogenates was recorded and expressed on a DNA basis (Fig. 1). The rate of incorporation was linear for at least 90 min. Attempts were made to increase the rate of $^{35}SO_4^{2-}$ incorporation by raising the concentration of nonradioactive sulfate in the medium, on the assumption that the concentration obtained with carrier-free $^{35}SO_4^{2-}$ might not be optimal. Little difference was found at low concentrations of nonradioactive SO_4^{2-} (0.6–60 μM), but at higher concentrations $^{35}SO_4^{2-}$ incorporation was decreased (by isotope dilution). At 0.12 mM SO_4^{2-} and 1.2 mM SO_4^{2-} (the last is the regular concentration in KRB), the decrease reached 58 and 84%, respectively. Consequently, all subsequent labeling was carried out with carrier-free $^{35}SO_4^{2-}$ (0.1–1.0 mCi/ml) in SO_4^{2-}-free KRB.

L-[4,5-^{3}H]leucine was used at 5 μCi/ml. Radioactive media were filtered through a 0.22-μm Millipore filter before use.

(e) Counting Procedure

Fractions were neutralized (when necessary), dis-

solved in scintillation fluid (0.3% 2,5-diphenyloxazole [PPO], 0.02% 1,4-bis[2-(5-phenyloxazolyl)]benzene [POPOP] wt/vol in 25% Triton X-114 vol/vol in xylene [4]), and counted in a Beckman LS 350 liquid scintillation spectrometer (Beckman Instruments, Inc., Fullerton, Calif.).

(f) Cell Fractionation

Minilobules were labeled for 1 h, rinsed three times with nonradioactive, complete KRB, and subsequently chased in the same solution for 45 min. At the end of the chase, they were collected by low speed centrifugation (150 g × 1 min), washed three times with cold 0.3 M sucrose, and then homogenized in the last solution using four strokes of a Teflon-glass Brendler type homogenizer (type A, 0.10–0.15 mm clearance, Arthur H. Thomas Co., Philadelphia, Pa.), driven at 3,000 rpm. The ensuing homogenate was filtered through 75-μm nylon cloth (Nitex, E. Tobler Co., New York) and zymogen granules were isolated from the filtrate by the procedure of Jamieson and Palade (20). The fractions were surveyed by electron microscopy and assayed for incorporated $^{35}SO_4^{2-}$ by autoradiography and radiochemical assays. In some experiments, performed to ascertain whether or not there was contamination of zymogen granule fractions by particles coming from other sources in the tissue (e.g. duct cells), the potential for contamination was maximized by not removing the duct fragments from the minilobule preparations before the latter's labeling and cell fractionation. No additional particulate contaminants were recognized
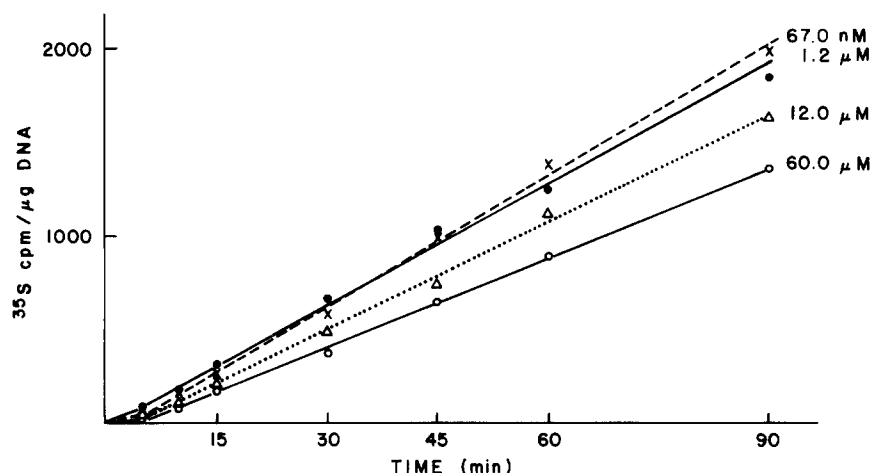

FIGURE 1   Kinetics of in vitro $^{35}SO_4^{2-}$ incorporation by pancreatic minilobules (guinea pig). Minilobules, prepared by collagenase treatment and washed three times in SO_4^{2-}-free KRB, were incubated in the same medium to which 100 μCi/ml $^{35}SO_4^{2-}$ (final SO_4^{2-} concentration: 0.067 μM) was added either alone or together with nonradioactive SO_4^{2-}. In the latter case, the final SO_4^{2-} concentrations ranged from 1.2 to 60.0 μM. At the times indicated, lobules were collected, homogenized, and fractionated by TCA precipitation. TCA-insoluble ^{35}S-radioactivity was determined and normalized to DNA content. Three additional experiments (two with fewer time points) gave similar results.

by electron microscopy or autoradiography in the corresponding fractions, and negligible contamination was detected by radiochemical assay.

(g) Subfractionation of Zymogen Granules

The mitochondrion-rich upper half of the zymogen granule pellet was removed by repeated surface rinsing with 0.3 M sucrose. The lower half, which consists primarily of zymogen granules (see Table IV) was resuspended in 40 mM NaCl-125 mM NH_4HCO_3, a solution in which the granules lysed. To recover the granule membranes (as a pellet), the lysate was centrifuged for 60 min at 105,000 g.

(h) Mixing Experiments

Mixing experiments were carried out to assess the extent of relocation of ^{35}S-labeled compounds liberated during homogenization from ruptured zymogen granules, Golgi elements, or other intracellular or extracellular compartments. To this intent, [3H]leucine-labeled minilobules were homogenized in a postmicrosomal supernate (105,000 g × 30 min) obtained from a separate but identical preparation labeled with [35]SO$_4^{2-}$. The degree of contamination of the zymogen granule fractions isolated from such homogenates was assessed by radiochemical assays and autoradiography.

(i) Microscopy

Tissue specimens were fixed with 1% OsO_4 in 0.1 M Na cacodylate buffer, pH 7.4, for 2 h at 4°C. Zymogen granule pellets were fixed for 3 h at 4°C directly in the centrifuge tube with 1% OsO_4 in 0.3 M sucrose (unbuffered, pH 5) (28). The mitochondrial layer was not washed out from the top of these pellets in order to increase the changes of detecting potential, ^{35}S-labeled particulate contaminants at that level. Microsomal pellets were fixed overnight in the same fixative. Some specimens were stained en bloc for 1 h in 0.5% Mg uranyl acetate in 0.9% NaCl before dehydration. All specimens were dehydrated in graded ethanols and embedded in Epon. While in 100% ethanol, the pellets were cut with a razor blade through the middle, and processed to allow systematic sectioning from top to bottom as described by Tartakoff and Jamieson (45). Thick sections were stained with 1% toluidine blue in 1% Na borate (35) and photographed with a Zeiss photomicroscope II. Thin sections, cut with a diamond knife on a Sorvall MT-2 ultratome, were doubly stained with uranyl acetate and lead citrate (48), and finally examined in a Siemens Elmiskop 102 EM.

(j) Autoradiography

Specimens for EM autoradiography were prepared by the loop technique (12), or by the flat-specimen procedure (37) using the Ilford L4 emulsion. In both cases, the sections were ~800 A thick (gold interfer-

ence color) and the emulsion layers ~1,000 A (purple interference color). After appropriate exposure, the preparations were developed with Microdol X (Eastman Kodak Co.). Specimens for LM autoradiography were dipped in Ilford L4 emulsion, exposed, and finally developed in D19.

Quantitative analysis of the autoradiographic grain density was performed as follows: For each experimental time point, sections obtained from two to three blocks were used, and low magnification (× 3,000) micrographs were taken at random from a single section on each grid until a sample of adequate size was obtained. For EM autoradiography, grain and point distributions were determined either on appropriately enlarged prints or on contact printed positive transparencies (made on Kodak EM film) which were examined in a stereological enlarger at × 5. Autoradiographic grains were assigned to different subcellular structures by the circling procedure used by Salpeter and Mc-Henry (39) for simple grain density analysis. Grains over the profiles of each type of subcellular component were counted directly on prints or projected images, and surface density for each type of component was determined on the same fields by established stereological procedures (49). The collected data were used to determine both simple grain density and percent distribution of label for different subcellular components.

(k) Gel Electrophoresis Procedure

Sodium dodecyl sulphate (SDS)-polyacrylamide gel electrophoresis was performed in 1-mm thick slabs using Neville's discontinuous system (32). The separating gel was a 5-15% continuous gradient of acrylamide (acrylamide:N,N'-methylene bisacrylamide, wt/wt 30:0.8). Protein samples were reduced and carboxymethylated as follows: To 50 µl of zymogen granule extract, 5 µl of 1 M Na_2CO_3, 10 µl of 20% SDS, 5 µl of freshly prepared 0.2 M dithiothreitol, and 5 µl of 0.1 M ethylenediaminetetraacetate (EDTA) were added; the mixture was heated to 100°C for 1 min and then mixed with 5 µl of 1 M iodoacetamide, 15 µl of 60% sucrose, and 5 µl of 1% bromophenol blue. After clearing the mixture by centrifugation, 5- to 50-µl samples were loaded on the gels and the latter were run for 8 h at 15 mA. At the end of the run, the gels were stained with 0.25% Coomassie Brilliant Blue in 30% methanol-7% acetic acid for at least 6 h, and destained in the same methanol-acetic acid solution for 24 h. For radioactivity assays, the gels were cut into 1-mm slices, and each slice was dissolved (for 24 h at 50°C) in 0.5 ml 30% H_2O_2 and counted as already described.

(l) Gel Filtration

The soluble molecules of the zymogen granule extract were fractionated by gel filtration on Sephadex G 150 and Sepharose 4 B columns (2.5 × 140 cm) which

were equilibrated and then dveloped at ~4°C with either 100 mM NH₄HCO₃, pH 8.3 (usual procedure), or 100 mM NH₄HCO₃-500 mM NaCl, pH 8.3 (high salt). The flow rates used were 30 ml/h and 17 ml/h for the Sephadex G 150 and Sepharose 4 B columns, respectively. The effluents were monitored for ultraviolet absorption and radioactivity. Ribonuclease, myoglobin, STI, ovalbumin, albumin, and aldolase were used as calibration standards.

From the Sephadex G 150 column a high molecular weight ^{35}S-labeled peak was isolated. The corresponding fractions were pooled, lyophilized and redissolved in 0.25 M tris(hydroxylmethyl)aminomethane (Tris)-HCl buffer, pH 8.0, containing 0.3 M Na acetate, 0.25 M NaCl, and 0.5 mg/ml BPA. Centrifugation of the ensuing solution gave a small precipitate, but 100% of the ^{35}S-counts were recovered in the supernate.

(m) Chemical Assays

DNA was determined in hot TCA extracts by Burton's (11) procedure using calf thymus DNA as standard.

Amino acids and amino sugars were analyzed with a Durrum 500 autoanalyser (Durrum Instrument Corp., Sunnyvale, Calif.). Uronic acids were determined by the carbazole reaction of Bitter and Muir (9) with glucuronolactone as standard. Heparan sulfate was characterized by 0.04 N HCl hydrolysis and nitrous acid treatment according to Kraemer (25). Chrondroitin sulfate was estimated by specific hydrolysis with chrondroitinase ABC according to Saito et al. (36). In both cases, cleavage products were analyzed by gel filtration on Sephadex G25 fine, or Sephadex G150 columns (0.9 × 50 cm), using 0.1 M ammonium acetate, pH 7.0, as eluant.

Materials

Materials were obtained from the following sources: Acrylamide, N,N'-methylenebisacrylamide, N,N,N',N', tetramethylethylenediamine, and sucrose from Eastman Kodak Co. (Rochester, N. Y.); ammonium persulfate, dithiothreitol, iodoacetamide, Trizma base, bromophenol blue, aldolase, ribonuclease, ovalbumin, carbazole, uronic acid, D-glucuronolactone, and SDS from Sigma Chemical Co. (St. Louis, Mo.); BPA from Armour Pharmaceutical Co. (Phoenix, Ariz.); calf thymus DNA, pure collagenase (batch CLSPA 54 K 405), and STI from Worthington Biochemical Corp. (Freehold, N. J.); carbamylcholine, myoglobin, L-[4,5-³H]leucine 59 Ci/mmol from Schwarz/Mann Div., Becton, Dickinson & Co. (Orangeburg, N. Y.); H₂^{35}SO₄ Carrier-free, PPO, and POPOP from New England Nuclear (Boston, Mass.); Triton X-114 from Rohm and Haas Co. (Philadelphia, Pa.); Sephadex G 10, G 150, and Sepharose 4 B, from Pharmacia Fine Chemicals (Piscataway, N. J.); and chondroitinase ABC (from *Proteus vulgaris*), from Seikagaku Fine Bio-

chemicals (Tokyo, Japan). All other chemicals were reagent grade.

RESULTS

1. Sites of Synthesis of Sulfated Compounds in the Guinea Pig Pancreas

The sites of ^{35}SO₄$^{2-}$ incorporation and accumulation (post-transport) were localized by LM and EM autoradiography using minilobules and dissected or isolated duct segments. Minilobules were preferred to usual lobules since in their case the autoradiographic grains were evenly distributed throughout the tissue. ^{35}SO₄$^{2-}$ incorporation was found to proceed at such a low rate in the guinea pig pancreas that short pulse labeling was not practical, and long exposures (60 min) to high concentrations of radioactive precursor (~1 mCi/ml) were needed to obtain an adequate autoradiographic response, especially in acinar cells.

(a) LM Autoradiography

LM autoradiographs were particularly useful in showing that ^{35}SO₄$^{2-}$ was incorporated not only in acinar cells, but also (at about the same rate) in the epithelium of small intralobular and interlobular ducts (Fig. 2b and d) and (at noticeably higher rates) in the epithelium of the major ducts of the gland (Figs. 2a and c, and Fig. 3). The ductal epithelium has a minority population of goblet cells which is restricted to the main collecting duct and its immediate affluents and is distributed in small clusters or in small accessory glands (Fig. 2a). Autoradiographs of major ducts labeled for 10-60 min with ^{35}SO₄$^{2-}$ indicated that the epithelium was generally and diffusively labeled; grain concentrations could be recognized only in a supranuclear position (presumably the Golgi region) in regular duct epithelia, and at the bottom of the calices in goblet cells (Figs. 2c and 3). After 60-min labeling, a substantial fraction of the label appeared over the periphery of the duct lumina (Figs. 2c and 3); at this time most of the autoradiographic grains associated with goblet cells were still over the bottom of their calices, suggesting that transport of their secretory products (mucus) was relativaly slow and that the luminal label was not necessarily over discharged mucus. The labeling of other cells and extracellular structures associated with the major ducts (Fig. 3) was either moderate (fibroblasts, connective tissue matrix)

or negligible (smooth muscle cells of the duct wall, nerve fibers, and blood vessels).

(b) EM AUTORADIOGRAPHY

SMALL DUCTS: In specimens exposed to $^{35}SO_4{}^{2-}$ for 1 h, the autoradiographic grains were found concentrated over the Golgi complex and the plasmalemma of the epithelial cells (Figs. 4 and 5). All plasmalemmal domains were labeled, but the luminal front was more heavily marked than the rest. These cells contained no labeled, morphologically recognizable secretory granules; they had, however, in their apical regions small vesicles (with a light content) which might transport labeled products from the Golgi complex to the luminal surface.

MAJOR DUCTS: The Golgi complex and the plasmalemma of the regular epithelial cells of these ducts appeared already labeled at the end of a 10-min pulse. After 60-min labeling, autoradiographic grains were found concentrated over the luminal plasmalemma and its microvilli, and after a subsequent chase of 30-60 min they began to appear over the periphery of the duct lumen. Some of the epithelial cells of these ducts have a few dense granules (reminiscent of secretory granules in other cell types), which appeared to be labeled (Fig. 6); yet the labeling affected the entire epithelial cell population, irrespective of the presence or absence of putative secretory granules. The labeling pattern was the same in isolated ducts or in ducts found in lobule preparations.

In general, the duct epithelium was found to be surprisingly active in $^{35}SO_4{}^{2-}$ incorporation, its activity increasing sharply with the size of the ducts and their proximity to the intestinal terminus. The chemical nature of the sulfated molecules produced by the duct epithelium is unknown (sulfated glycolipids? sulfated glycoproteins?), but since they represent a potential source of sulfated compounds in the discharged secretion and of contaminants in cell fractions, duct fragments were systematically and carefully removed from minilobule preparations in subsequent experiments.

ACINI: After 60-min exposure to $^{35}SO_4{}^{2-}$, autoradiographic grains were found concentrated over Golgi elements (i.e., piled Golgi cisternae and associated Golgi vesicles), Golgi condensing vacuoles, and zymogen granules in the apical region of acinar cells (Figs. 7 and 8). The labeling of these compartments, to be referred to hereafter as "distal secretory structures," was expected in view of the findings of Berg and Young (8) on mouse pancreatic acinar cells, but in the guinea pig pancreas other subcellular components of the exocrine cells, especially the rough endoplasmic reticulum (RER), also appeared to be labeled.

The distribution of autoradiographic grains over various intracellular compartments was determined as indicated under Materials and Methods (section j), the RER being arbitrarily divided into a basal and an apical part to allow an assessment of radiation spread from the distal secretory structures (the main source of ^{35}S-radioactivity) to neighboring RER elements. Radiation spread should be maximal in the apical region, given its internal geometry, the energy of the emitted particles, and the distances over which they are expected to be scattered. The half distance (HD) (i.e. the distance within which half of the autoradiographic grains are expected to fall) has not been established experimentally for a ^{35}S-radiation source, but it is estimated to be similar to that determined for a ^{14}C-source (40), which — under our experimental conditions — would be ~2,300 Å. With this in mind, the two parts of the RER were separated by tracing on each micrograph a boundary at 2 HD (0.46 μm) from any distal secretory structure (Fig. 7). All RER elements falling within this boundary (or between this boundary and the cell's apex) were considered apical; those beyond the boundary were considered basal.

Table I gives the grain distribution, the surface density of the different compartments, and the ratio grains/μm^2 for each compartment. It should be pointed out that an important cell compartment, the cytoplasmic matrix, could not be included in the list of structures or compartments analyzed because of the low resolution of the autoradiographic technique. The cytoplasmic matrix was arbitrarily apportioned to the other compartments, primarily to the RER.

Of the total number of grains counted (1,910), ~47% appeared over the distal secretory structures of the acinar cells, ~45% over their RER (and associated cytoplasmic matrix), and ~8% over other structures (mitochondria and nuclei). Grain concentration per unit area was the highest over Golgi elements and condensing vacuoles, and higher in general over distal secretory structures than over other cell compartments. As expected, the grain concentration was higher
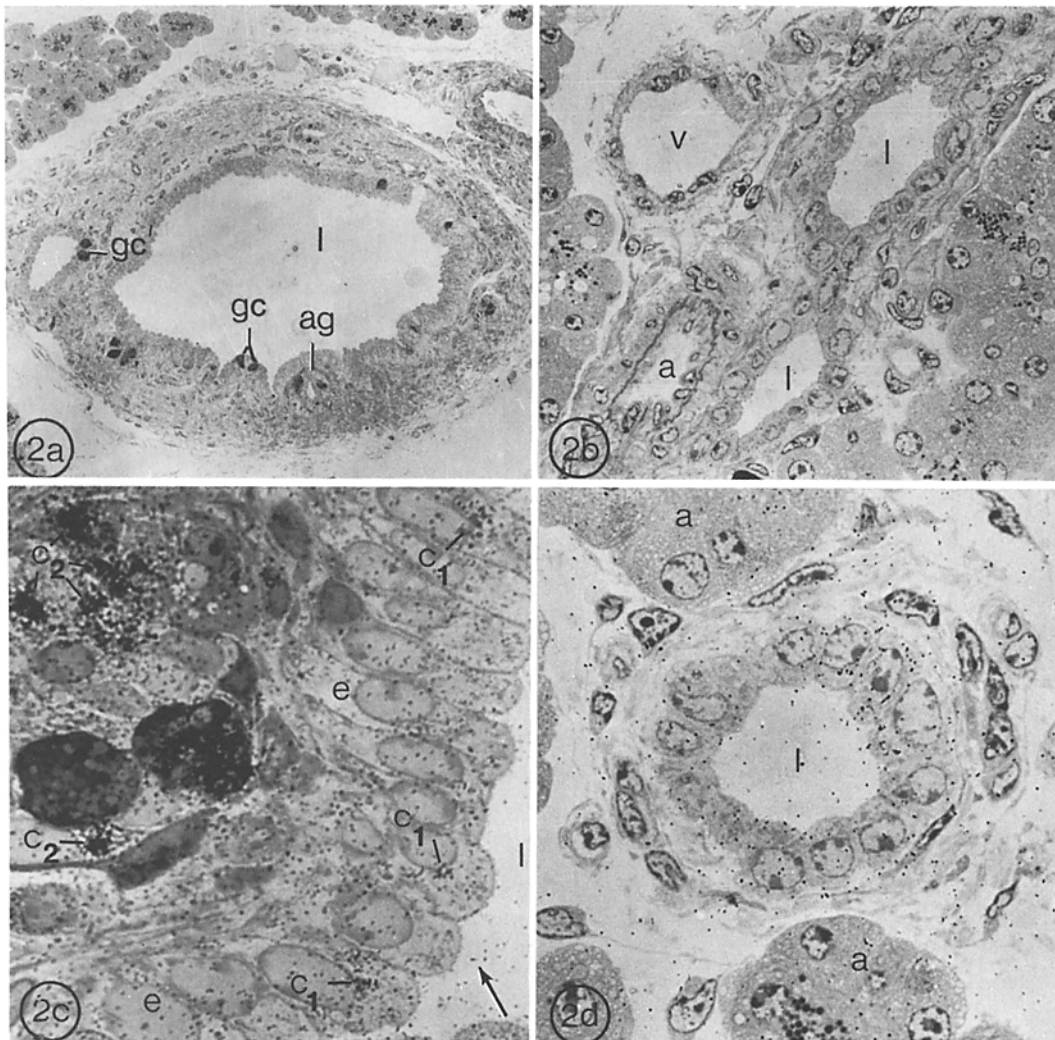
FIGURES 2 and 3   Gallery of LM autoradiographs taken at different levels along the collecting duct system of the pancreas. For all these figures, the exposure of the tissue to label lasted 60 min and the exposure of the autoradiographs was extended for 21 days.

FIGURE 2   (a) Main duct at low magnification to illustrate the presence of accessory glands (ag) and of scattered goblet cells (gc) in the epithelium. Note the presence of goblet cells (gc') in an immediate affluent of the main duct. l, duct lumen. × 200. (b) Interlobular duct (obliquely sectioned) located at the periphery of a lobule and associated with blood vessels. l, Duct lumen; a, artery; v, vein. Note the reduction in thickness of both the wall and epithelium of the duct. × 500. At the magnifications used in Fig. 2a and b, autoradiographic grains are not visible. (c) Same duct as in Fig. 2a. Small field magnified to illustrate the presence of autoradiographic grains (in high concentration) over the epithelium (e) and (in lower concentration, arrow) over adjacent regions in the lumen (l). The clusters of autoradiographic grains at c_1 probably mark Golgi complexes in ductal epithelial cells, those at c_2 mark the base of the calyx in goblet cells. × 1,150. (d) Higher magnification of a cross section through a small interlobular duct. Autoradiographic grains are present at low concentration over the epithelium, the lumen (l), and surrounding connective tissue; a, pancreatic acini. × 1,000.
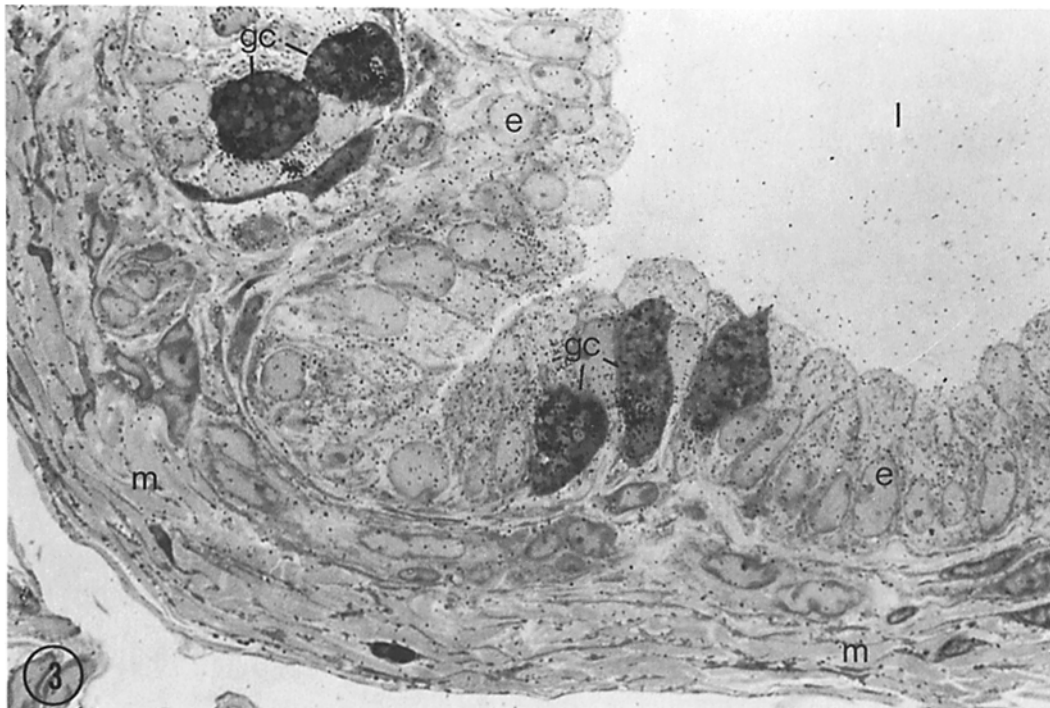
FIGURE 3   Different section through the same duct as in Fig. 2a and e. This large field illustrates the extensive labeling of the epithelium (e) including its goblet cells (gc), the less extensive labeling of the other elements in the duct wall, primarily smooth muscle cells (m), and the presence of autoradiographic grains over the lumen (l). × 1,000.
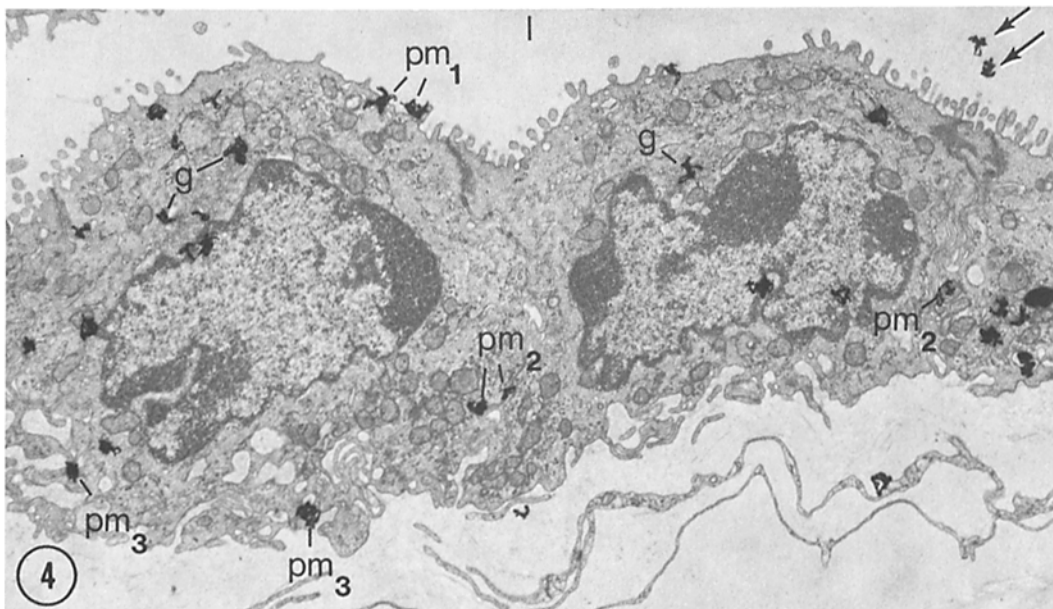

FIGURE 4   EM autoradiograph of epithelial cells in an intralobular duct labeled in vitro with $^{35}SO_4^{2-}$ (1 μCi/ml) in sulfate-free KRB. Most of the autoradiographic grains mark either the Golgi complexes (g), or the plasmalemma on the luminal (pm_1), lateral (pm_2), or basal (pm_3) aspects of the cells. Few grains (arrows) are found over the lumen. × 9,000.
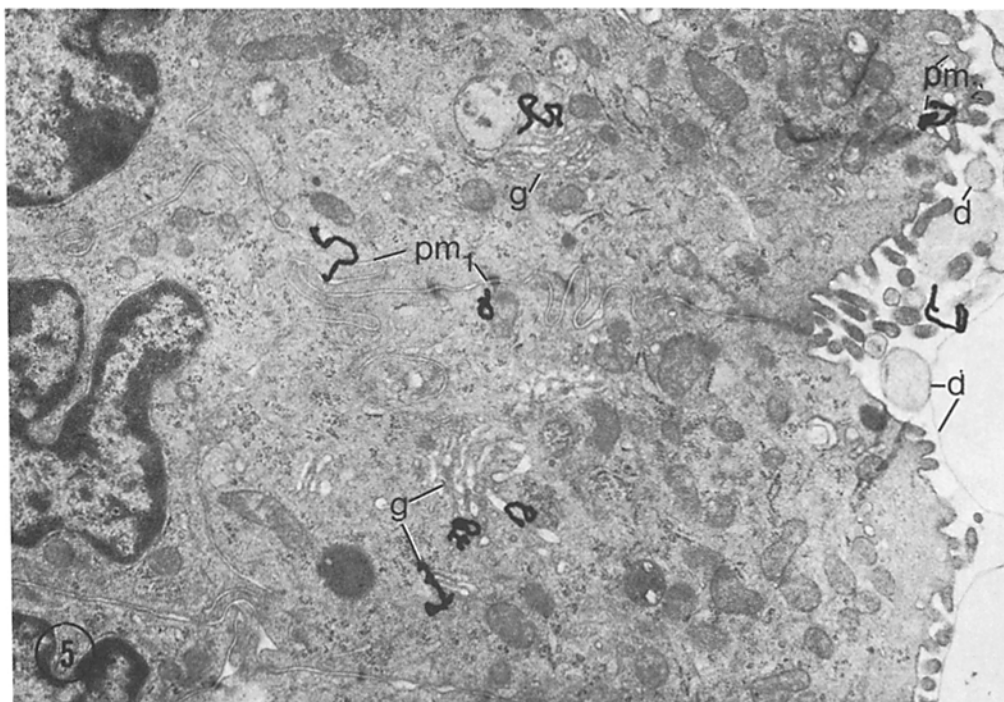
FIGURE 5 EM autoradiograph of epithelial cells in an interlobular duct fragment labeled in vitro, as for Fig. 4. The autoradiographic grains mark the Golgi complexes (g) of two adjacent cells, and their luminal (pm_2) and lateral (pm_1) plasmalemmal domains. Detritus (d) often marks the lumen in such preparations. × 8,000.

over the apical part of the RER than over the basal part of the system. If the difference between the two parts of the RER were attributed entirely to radiation spread from Golgi elements, condensing vacuoles and zymogen granules, and if the grain distribution were corrected for the assumed spread, then the percentage of grains over distal secretory structures would rise to ~60% of the total. This corrected figure represents most likely a minimal value, since not more than 75% of the grains generated by sources at the periphery of the apical region are expected to fall within the boundaries traced by us, and since, for the sake of expediency, we have assigned grains to structures as done for simple density analysis, rather than by more laborious procedures which could provide a better assessment of radiation spread (39).

When the $^{35}SO_4^{2-}$ label was chased for 60 or 180 min (after a standard 60 min incorporation), the distrbution of autoradiographic grains changed with time as shown by the data in Table II. There was progressive increase in concentra-tion and progressive accumulation of grains over zymogen granules (from ~10% at the end of the labeling to ~33% at the end of the longest chase). Fig. 10 illustrates the heavy concentration of grains over zymogen granules after a 180-min chase; part of the grains seem to be associated with apical smooth-surfaced vesicles, and possibly with the luminal plasmalemma. There was also a continuous complementary decrease in the percentage of grains over Golgi elements (from ~24% at the end of the incubation to ~7% at the end of the 3-h chase), with a rapid decrease in concentration. Fig. 8 illustrates the concentration of grains over Golgi elements (stacked cisternae and small vesicles) at the end of the labeling period. The percentage of grains over condensing vacuoles also declined, but only after reaching an apparent peak after 1-h chase (Fig. 9). The percentage of grains over all distal secretory structures (considered together) showed much less variation: it hovered between 45 and 50%, with a slight but continuous decrease in average concentration. According to these data,
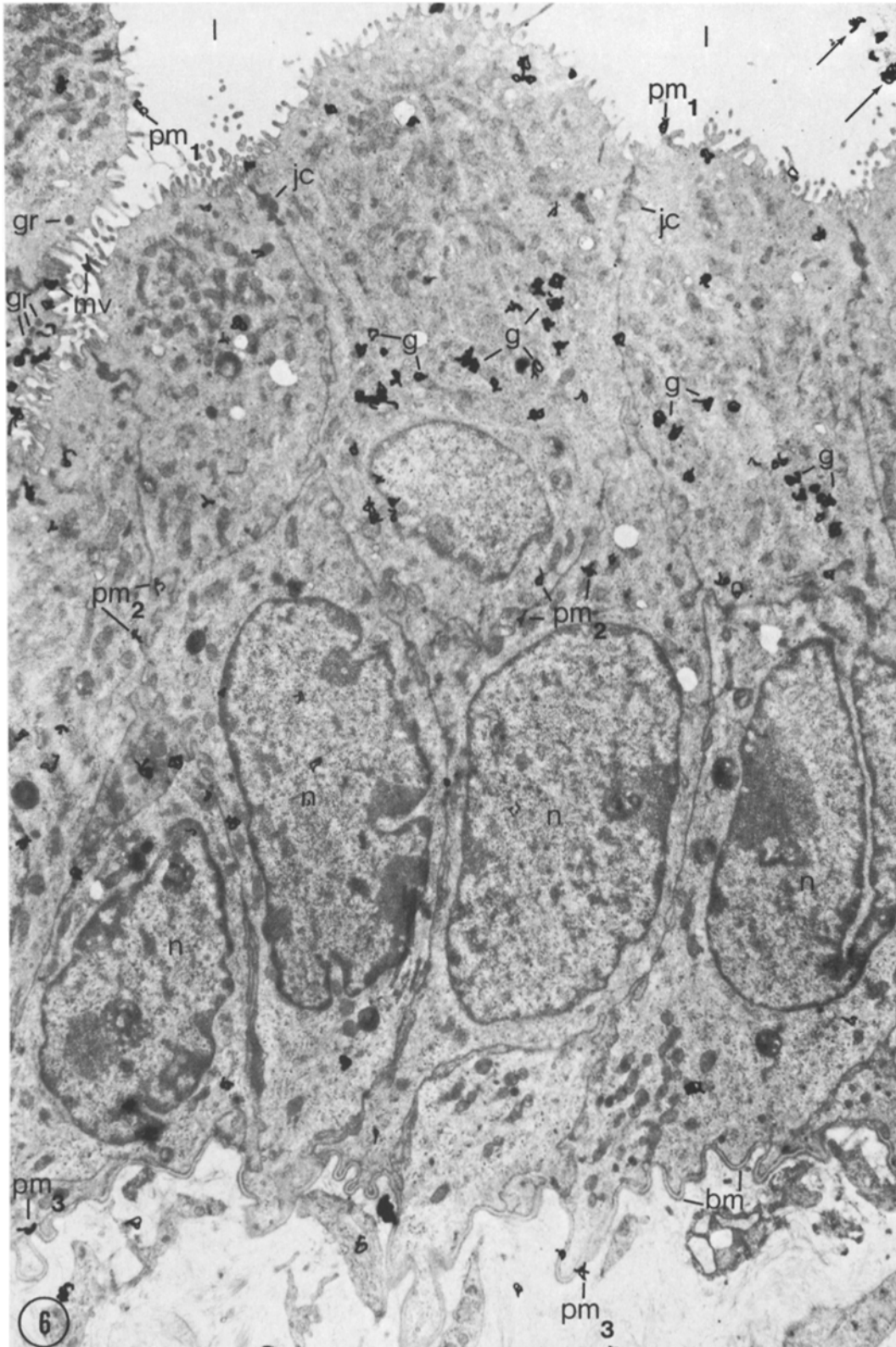
FIGURE 6   EM autoradiograph of epithelial cells in a major pancreatic duct (main duct or immediate affluent). Dissected specimen incubated for 60 min in $^{35}SO_4{}^{2-}$ (1 mCi/ml) in sulfate-free KRB. Most of the grains are clustered over Golgi complexes (g), luminal (pm_1), lateral (pm_2), and basal (pm_3) plasmalemma, and microville (mv) of the luminal cell front. gr, granules (possibly secretion granules); l, duct lumen, (the arrows point to labeled cellular detritus in the lumen); jc, junctional complexes; n, nuclei; bm, basement membrane. × 6,500.
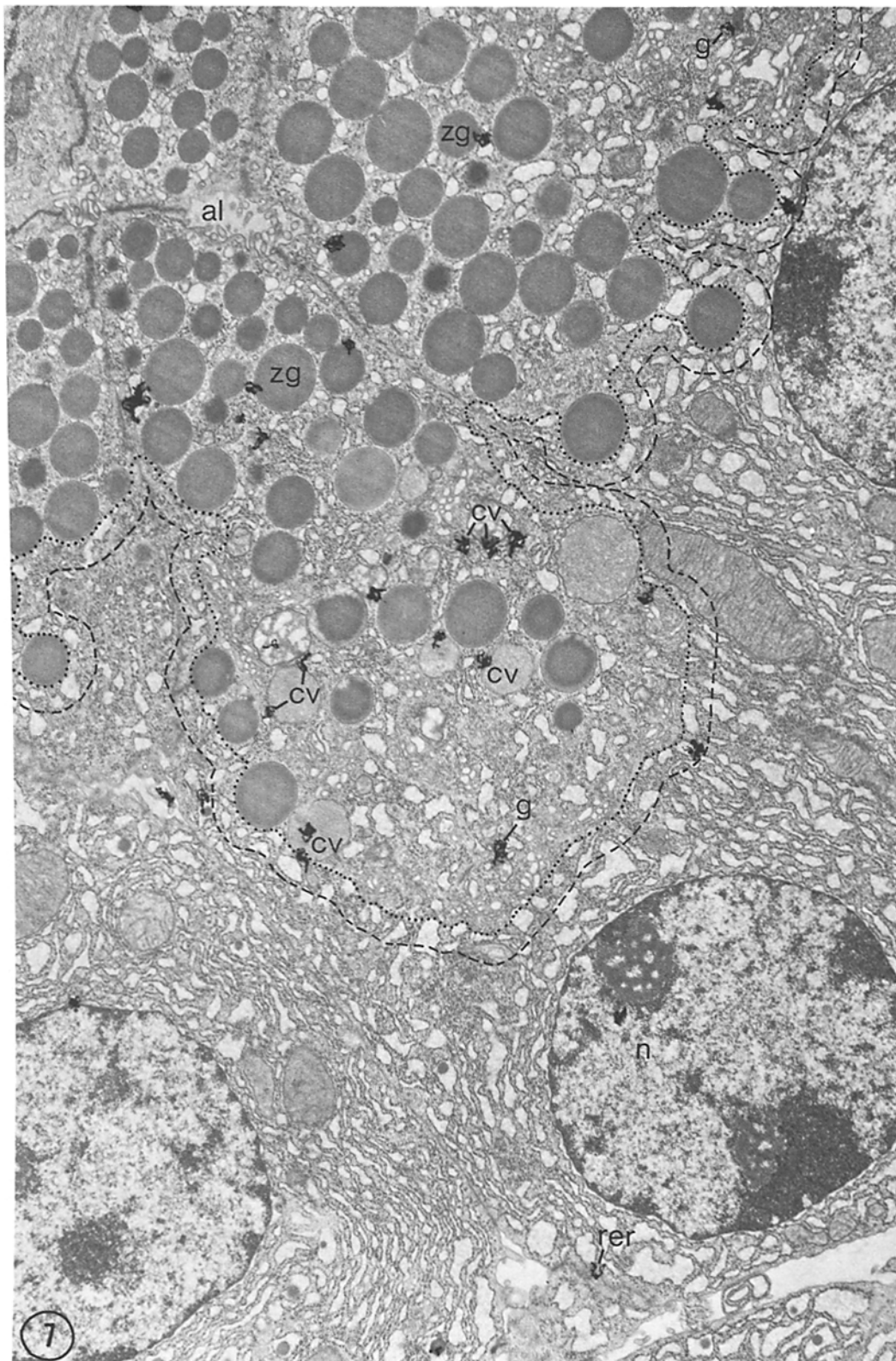
FIGURE 7 EM autoradiograph of acinar cells from a minilobule preparation labeled in vitro for 60 min with $^{35}SO_4^{2-}$ (1 mCi/ml). The autoradiographic grains are concentrated over condensing vacuoles (cv), Golgi stacks (g) and zymogen granules (zg). There are few grains over other structures, e.g., rough endoplasmic reticulum (rer) and nuclei (n). Acinar lumina are marked al. The dashed line is the boundary between the apical and basal domains of the RER. It is traced at 2 HD (0.46 μm) of the point line which follows the proximal limit of all distal secretory structures. × 8,500.
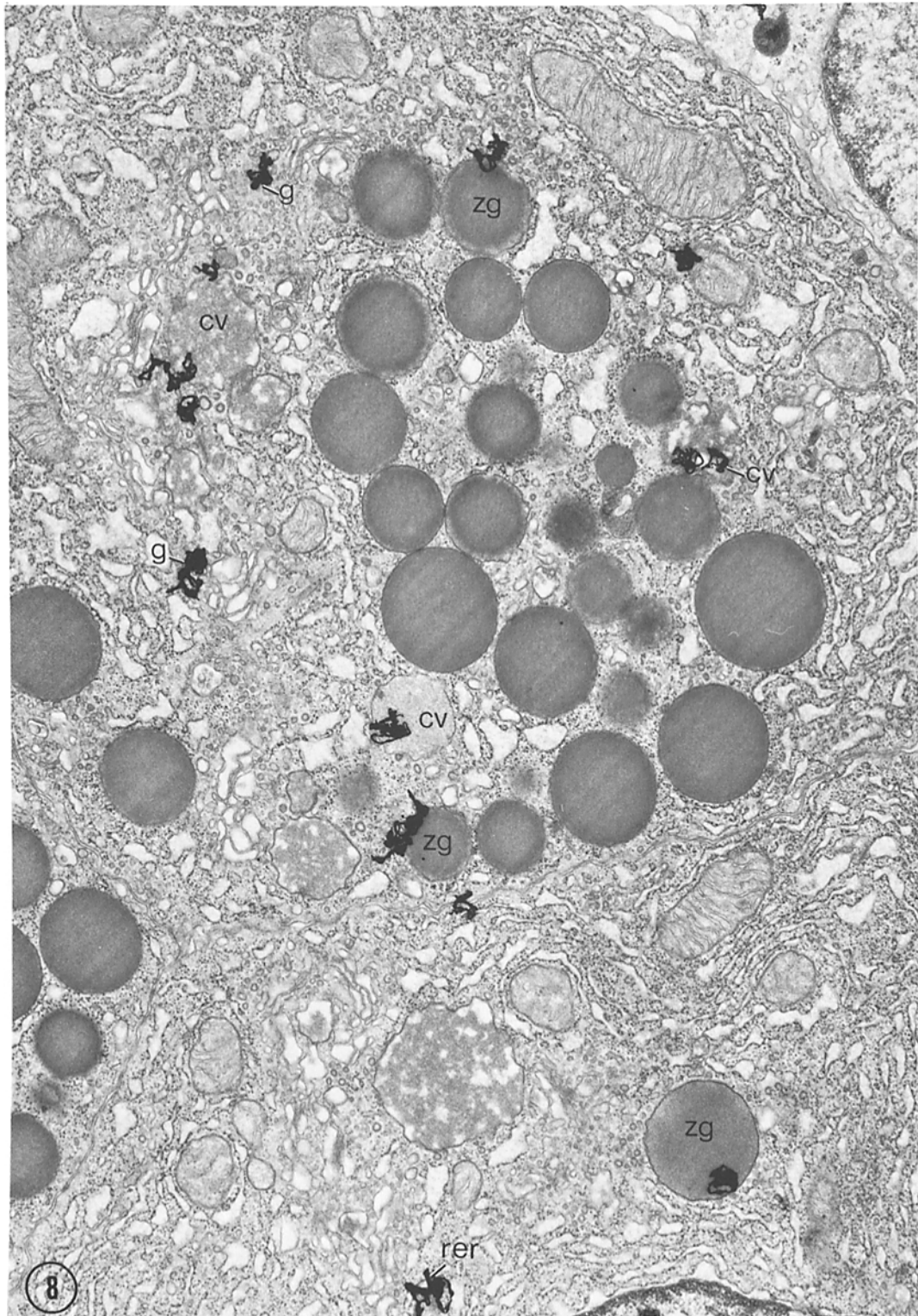
FIGURE 8   EM autoradiograph of an acinar cell in a minilobule preparation labeled in vitro as for Fig. 7. Most of the autoradiographic grains are located over Golgi elements (*g*) and condensing vacuoles (*cv*) with content in different phases of concentration. Some grains are found over or near zymogen granules (*zg*). Few grains are seen over the RER (*rer*) and other structures. × 17,500.

TABLE I

Distribution of Autoradiographic Grains over Pancreatic Acinar Cells Labeled for 60 min with $^{35}SO_4^{2-}$

Compartments examined	Grains counted	Grains	Area	Grains/μm^2
		%	%	
Zymogen granules	187	9.8	8.2	0.11
Condensing vacuoles	236	12.4	3.5	0.34
Golgi elements	471	24.6	6.9	0.34
Total distal secretory structures		46.8 (+11.5)*	18.6	
RER, basal	469	24.6	48.1	0.05
RER, apical	397	20.8 (−11.5)*	18.1	0.11
Total RER		45.3	66.2	
Mitochondria	74	3.9	5.8	0.064
Nuclei	76	4.0	9.4	0.041
Total Acinar cells	1,910	100	100‡	0.10

Pancreatic minilobules were prepared, labeled in vitro with $^{35}SO_4^{2-}$ (1 mCi/ml) for 60 min, and then fixed and processed for autoradiography by the flat specimen procedure as given under Materials and Methods, sections *i* and *j* (exposure time: 7 wk); autoradiographic grains were scored and related to unit areas as in section *j*. Data obtained in one experiment representative for a series of four.

* Estimated correction for radiation spread.

‡ Total points counted: 2,922.

TABLE II

Distribution of Autoradiographic Grains in Pancreatic Acinar Cells after $^{35}SO_4^{2-}$ Labeling (60 min) followed by Chase

Compartments examined	60 min Incorporation		+1 h Chase		+3 h Chase	
	% grains	grains/μm^2	% grains	grains/μm^2	% grains	grains/μm^2
Zymogen granules	9.9	0.11	14.2	0.12	33.4	0.15
Condensing vacuoles	12.3	0.34	19.3	0.31	8.6	0.14
Golgi elements	24.6	0.34	11.6	0.14	7.6	0.073
Total distal secretory structures	46.8 (+11.5)	0.24	45.1 (+16.1)	0.17	49.7 (+16.6)	0.13
RER, basal	24.6	0.048	22.3	0.04	17.4	0.032
RER, apical	20.8 (−11.5)	0.11	26.8 (−16.1)	0.11	28.1 (−16.6)	0.077
Total RER	45.3	0.066	49.1	0.065	45.5	0.05
Mitochondria	3.9	0.064	2.8	0.047	2.2	0.033
Nuclei	4.0	0.041	3.0	0.031	2.6	0.021
Total acinar cells		0.11		0.085		0.067
Total grains counted	1,910		1,908		1,885	
Total points counted	2,922		3,306		4,110	

Minilobules prepared and incubated as for Table I except that at the end of the 60-min labeling period, they were washed three times in KRB containing the usual concentration (1.2 mM) of nonradioactive SO_4^{2-}. At the end of the labeling and of each specified chase period, the minilobules were fixed and processed for autoradiography by the flat specimen procedure as given under Materials and Methods, section *i* and *j* (exposure time: 7 wk); autoradiographic grains were scored and related to unit area as indicated in section *j*. Data obtained in one experiment representative of a series of four. Variations in surface density for a given compartment from time point to time point were small and the average values were comparable to those reported by Bolender (10).

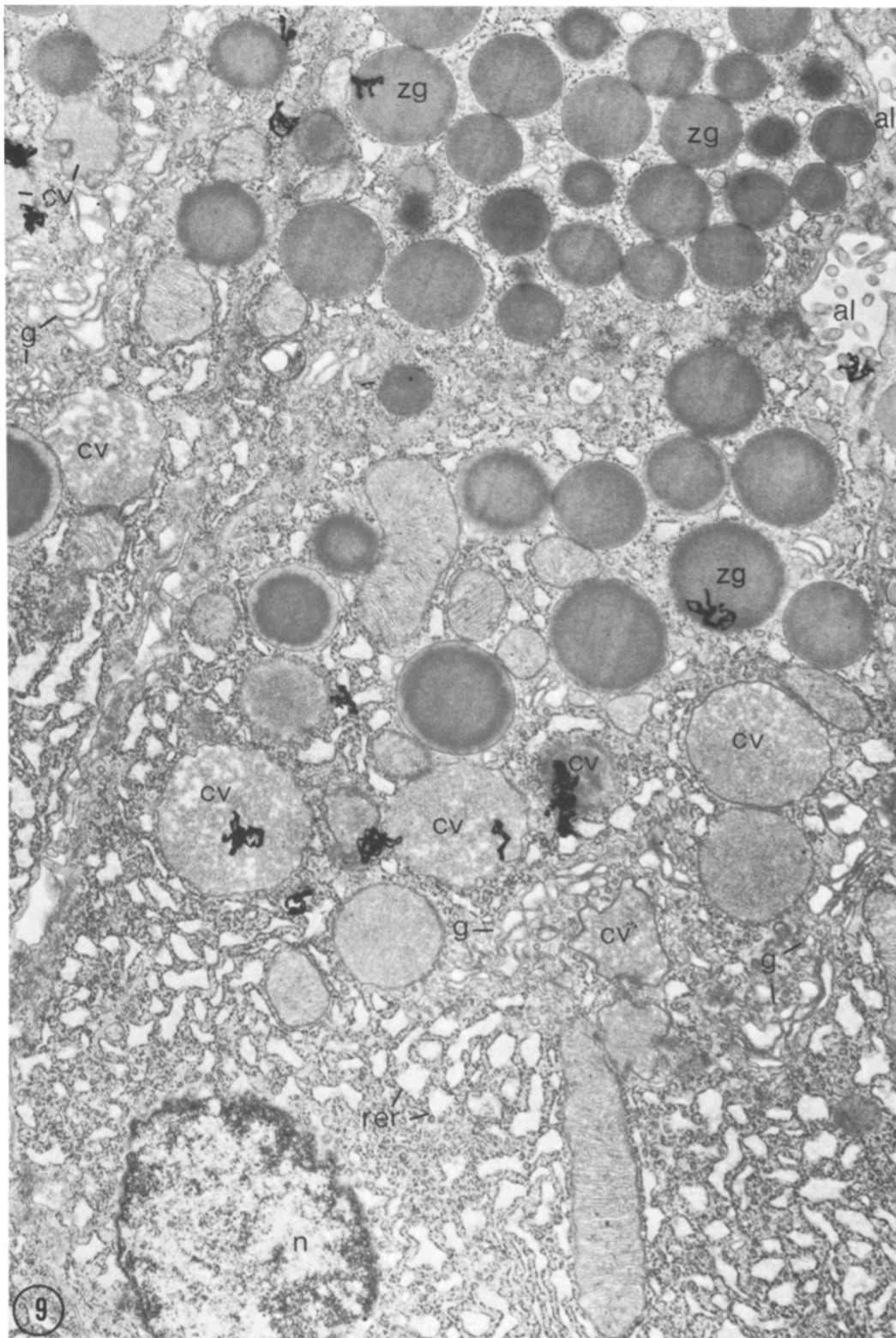FIGURE 9 EM autoradiograph of an acinar cell in a minilobule preparation labeled as for Figs. 7 and 8, then chased for 60 min in KRB containing nonradioactive sulfate. Most of the autoradiographic grains are located over condensing vacuoles (cv) and zymogen granules (zg). In this field, the Golgi cisternae (g) are not labeled. n, nucleus; rer, rough endoplasmic reticulum; al, acinar lumen. × 15,500.

the distal secretory structures showed a net loss rather than a gain in radioactivity over the chase period, during which the main event appeared to be the transport of a relatively large fraction of sulfated compounds from Golgi elements to zymogen granules.

The percentage of grains over the RER also showed little variation during the chase, but a clear difference appeared with time between the basal RER which showed a progressive loss in percent distribution and concentration, and the apical RER in which the situation was nearly reversed (increase in percentage with a slight decrease in concentration). These results can be explained by assuming (as already mentioned) that a substantial fraction of the autoradiographic grains found over the RER represent radiation spread from nearby distal secretory structures. The assumption is supported by the fact that 66–85% of the grains found over the apical RER fell within 2 HD from either condensing vacuoles or zymogen granules after a 1- or 3-h chase.

Some of the results obtained in our chase experiments deserve to be pointed out:

(a) The label was clearly chasable to zymogen granules, but the rate of transport seemed to be slower than for secretory proteins labeled with radioactive amino acids (cf. references 20 and 21): label still lingered in Golgi elements and condensing vacuoles after a 3-h chase.

(b) At all times, the concentration of grains over the basal RER (and associated cytoplasmic matrix) was 6–10 times lower than over condensing vacuoles; the same applied to nuclei and mitochondria.

(c) Although the RER lost label progressively, ~17% of the total grains was still found over the basal part of the system (and ~28% over its apical part) by the end of the 3-h chase. The nature of the sulfated compounds associated with the RER, and their relationship to the compounds present in the distal secretory structures are unknown.

(d) The acinar cells lost label continuously: the ratio grains/μm^2 over the entire cell area dropped from ~0.10 at the end of the incubation period to ~0.07 at the end of a 3-h chase. With the exception of the zymogen granules, all compartments lost label, but the highest losses were incurred by the distal secretory structures. A satisfactory explanation of the overall loss is not possible at present. Part of it may be ascribed to a progressive dilution of the intracellular $^{35}SO_4^{2-}$ pool; and part of it may reflect spontaneous

secretory discharge (cf. references 42 and 46), since a small number of grains (3–4% of the total) was regularly found over acinar lumina in chased specimens.

When a 3-h chase was carried out under continuous stimulation with 10^{-5} M carbamylcholine, the percentage of autoradiographic grains associated with distal secretory structures and apical RER dropped by ~40%. The most important losses (~60%) were recorded for the grains found over zymogen granules; the latter also showed, as expected, a substantial loss in aggregate volume (or surface density). The rest of the distribution pattern showed higher percentages of grains over the basal RER, mitochondria, and nuclei (than in the unstimulated controls), without increases in local concentrations (grains/μm^2).

Table III compares the labeling of acinar cells to that of islet cells (endocrine cells) and that of the epithelial cells of the intralobular ducts (centroacinar cells included). In the tabulated experiment, the concentration of grains over duct epithelial cells (which represents <10% of the lobule volume) was nearly the same as over acinar cells. In centroacinar cells, as in the duct epithelium, in general, the label was concentrated over the Golgi complex and the plasmalemma. The concentration of label was consistently higher over islet cells (primarily β cells) than over acinar cells. As in the latter, most of the grains were found over the Golgi complex and the secretion granules.

2. Sulfated Compounds in Zymogen Granule Fractions

(a) ISOLATION AND CHARACTERIZATION OF ZYMOGEN GRANULE FRACTIONS

The detection of active sites of $^{35}SO_4^{2-}$ incorporation in the duct epithelium, and the possibility that at least some of the corresponding products (mucus, for instance) were secreted, ruled out the use of discharged secretion as a reliable source for the isolation of the sulfated polyanions presumably involved in the concentration step of the cell's secretory products. Hence, we decided to isolate these compounds directly from zymogen granules.

Zymogen granule fractions were obtained from both unlabeled and $^{35}SO_4^{2-}$-labeled minilobules as given under Materials and Methods (section f).

MORPHOMETRY: The morphometry of zymogen granule fractions (Table IV) showed that >90% of the area occupied by particles in the bottom half of the corresponding pellets was taken
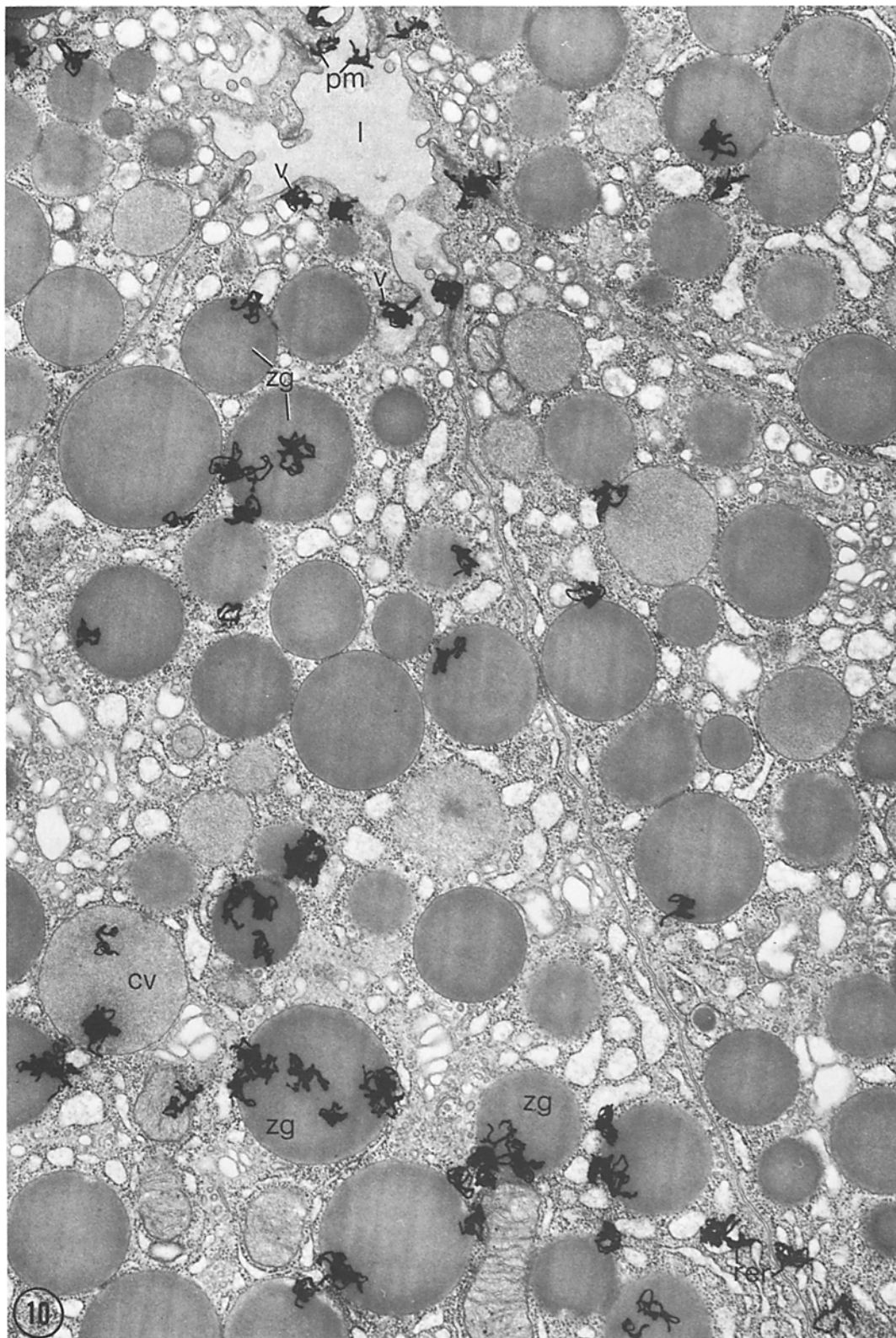
FIGURE 10   EM autoradiograph of an acinar lumen (*l*) and surrounding apices of exocrine cells. Minilobules labeled in vitro for 60 min with $^{35}SO_4{}^{2-}$ and then chased for 180 min in regular KRB. A few grains are still seen over a condensing vacuole (*cv*), but most of the others are marking zymogen granules (*zg*), and still others appear over smooth surfaced vesicles (*v*) in the vicinity of the lumen (*l*), and over the luminal plasmalemma (*pm*). Few grains are found over elements of the ER (*rer*). × 15,500.

by zymogen granules and condensing vacuoles, and the rest by mitochondria and rough microsomes (containing intracisternal granules). In the two upper quarters of the pellets, the corresponding value for zymogen granules dropped to ~60 and ~20%, respectively, while the area accounted for by mitochondria increased sharply to ~70% (in the top quarter), the rest being taken by additional contaminants, primarily lysosomes and rough microsomes (containing intracisternal granules).

AUTORADIOGRAPHY: Pellets of zymogen granule fractions, isolated from minilobules incubated with $^{35}SO_4^{2-}$ (1 mCi/ml) for 90 and 120 min, were processed for autoradiography without removing their upper layers in order to assess the distribution of ^{35}S-radioactivity in zymogen granules as well as in all the contaminants of the

fractions. Table IV gives the results of an analysis carried out on such a pellet at the three different levels described in the preceding section. In all layers, the highest percentages and the highest grain concentrations were found over zymogen granules and condensing vacuoles (Fig. 11 a and b). The mitochondria were less labeled and part of the grains associated with them could be ascribed to radiation spread from zymogen granules and condensing vacuoles. The increase in the specific radioactivity of zymogen granules in the upper layers of the pellet reflected local increases in the frequency of condensing vacuoles, while the increase in specific radioactivity over "other structures" in the top layer was due to the presence of heavily labeled lysosomes (Fig. 11 b). The analysis convincingly established the association of

TABLE III

Distribution of Autoradiographic Grains over Acinar, Ductal, and Endocrine Cells after 60 min Labeling with
$^{35}SO_4^{2-}$

Cell type	Point counts	Area	Grain counts	Grains	Grains/μm²
		%		%	
Acinar cells	10,338	91.6	5,703	90.6	0.081
Duct epithelial cells*	803	7.1	488	7.7	0.082
Endocrine cells‡	148	1.3	104	1.7	0.10

Minilobules prepared and processed as for Table I. Autoradiographic grains were counted and areas determined on acinar cells, epithelial cells of the intralobular ducts (including centroacinar cells), and endocrine cells. In two other experiments, the concentration of label over duct cells was slightly lower than over acinar cells.
* Cells of the epithelium of intralobular ducts, centroacinar cells included.
‡ In another experiment, in which 370 grains and 540 points were counted, the grain concentration was similar (0.11/μm²)

TABLE IV

Distribution of Autoradiographic Grains in a Zymogen Granule Pellet Isolated from $^{35}SO_4^{2-}$-Labeled
Minilobules (Guinea Pig Pancreas)

Component	A. Bottom half			B. Intermediary quarter			C. Top quarter		
	% grains	% area	grains/μm²	% grains	% area	grains/μm²	% grains	% area	grains/μm²
Zymogen granules (+ condensing vacuoles)	93.5	43.5*	0.182	81.9	30.4	0.240	41.7	8.7	0.232
Mitochondria	2.2	2.2	0.082	10.0	12.1	0.073	37.7	31.7	0.056
Other structures	1.5	1.5	0.082	3.0	8.7	0.071	10.5	4.2	0.120
Embedding matrix	2.8	52.8	0.005	5.0	48.8	0.007	10.1	55.4	0.007

Total number of grains counted: A, 324; B, 338; C, 228. Zymogen granules were isolated from minilobules labeled in vitro with 1 mCi/ml $^{35}SO_4^{2-}$ for 90 min and then chased in regular KRB for 45 min. The pellet was prepared for autoradiography without removing the top (mitochondrion-rich) layers. Autoradiographic grains were scored as given under Materials and Methods (section j), and the results are given for three different layers in the pellet. The bottom half of the pellet is the fraction used in subsequent preparative experiments. Data obtained in one experiment. A second experiment gave similar results.
* This area represents 92% of the total area occupied by particles in the bottom part of the pellet. The corresponding values for intermediary and top quarters are 59% and 20%, respectively.

newly synthesized sulfated compounds with zymogen granules, and showed that the potential contributions of such compounds from mitochondria and other contaminants was small and could be reduced to <10% by washing away the upper layers of the pellets. In fact, mitochondrial ^{35}S-radioactivity could be considered negligible, given the extent of radiation spread expected from label incorporated in zymogen granules.

The autoradiographs of the microsomal pellets were not quantitated. Their inspection suggested that a sizable fraction of the ^{35}S-label was associated with either lysosomes or Golgi elements (recognizable as Golgi cisternae); yet many grains appeared to mark usual rough microsomes. It is possible that part of the label is due to leakage from distal secretory structures followed by relocation by adsorption on microsomes (cf. footnote 2).

(b) Cell Fractionation of Doubly Labeled Minilobules

To gain more insight into the distribution of the sulfated compounds within zymogen granules, minilobules were incubated for 60 min in the presence of [³H]leucine (5 μCi/ml) and [35]SO_4^{2-} (100 μCi/ml), chased for 45 min, and then used as a starting material for the isolation of a zymogen granule fraction. At the end of the chase, most of the incorporated ³H-radioactivity (cf. reference 20) and a substantial fraction of the ^{35}S-radioactivity (Table II, in this paper) were expected to have arrived already in condensing vacuoles and zymogen granules, and hence to appear in an isolated zymogen granule fraction.

Table V shows that 28 and 21% of the TCA-precipitable ³H- and ^{35}S-radioactivities of the starting preparation, respectively, were actually recovered in the zymogen granule fraction. Removing the top layers of the corresponding pellets (by surface rinsing) reduced the recovery to 17% for [³H]leucine and 8% for [35]SO_4^{2-}. This nonparallel loss might be explained by extensive removal of [35]SO_4^{2-}-labeled condensing vacuoles and lysosomes together with the mitochondria of the upper layers of the pellets (see Table IV). The washed pellet was lysed and the membranes of the zymogen granules were recovered as given under Ma-

---

[2] Scheele, G. A., A. Tartakoff, and G. E. Palade. Leakage and relocation of secretory proteins during homogenization of pancreatic tissue. Manuscript submitted for publication.

terials and Methods (section g). In the experiment in Table V, the membrane pellet accounted for ~37% of ^{35}S-radioactivity, but only 5% of ³H-label of the granule lysate. In four other experiments, the corresponding value for ^{35}S-radioactivity was as high as 40-50%. About half of the ^{35}S-label could be removed from resuspended membrane pellets by either sonication or repeated extractions with lysis medium; the rest remained associated with the membranes.

At present, we do not know whether the easily extractable sulfated compounds are or are not different from those less readily removed, and we do not know either what the relationship is between, the latter and the membranes of the zymogen granules.

MIXING EXPERIMENTS: Sulfated compounds liberated during lobule homogenization from a variety of sources (duct epithelium, for instance) might be relocated by adsorption to the outer aspect of the membranes of zymogen granules. This possibility deserves special consideration in view of the possible association of the ^{35}S-label with the granule membranes. To check on this type of contamination by relocation, minilobules were labeled for 60 min with [³H]leucine, chased for 45 min, and then homogenized directly into a postmicrosomal supernate prepared by fractionating another set of minilobules previously labeled for 60 min with [35]SO_4^{2-} (see Materials and Methods, section h).

The distribution of TCA-precipitable ³H-radioactivity followed the usual pattern, but little ^{35}S-label was recovered in the corresponding zymogen granule fractions; moreover, most of it was removed (by surface washing) with the mitochondrion-rich top layers of the pellets. In the experiment in Table VI, only 0.6% of the TCA-precipitable ^{35}S-label was left in the bottom half of the zymogen granule pellet; in three other experiments, the corresponding values were 0.1% or less. Autoradiography of the same pellets showed no label (above background) associated with zymogen granule profiles. Taken together, these results suggest that, during tissue homogenization, relocation by adsorption of sulfated compounds on zymogen granules is negligible, if at all extant.

(c) Subfractionation of Zymogen Granule Extracts

The results so far presented, especially the autoradiographic findings, establish convincingly the presence of [35]SO_4^{2-}-labeled macromolecular
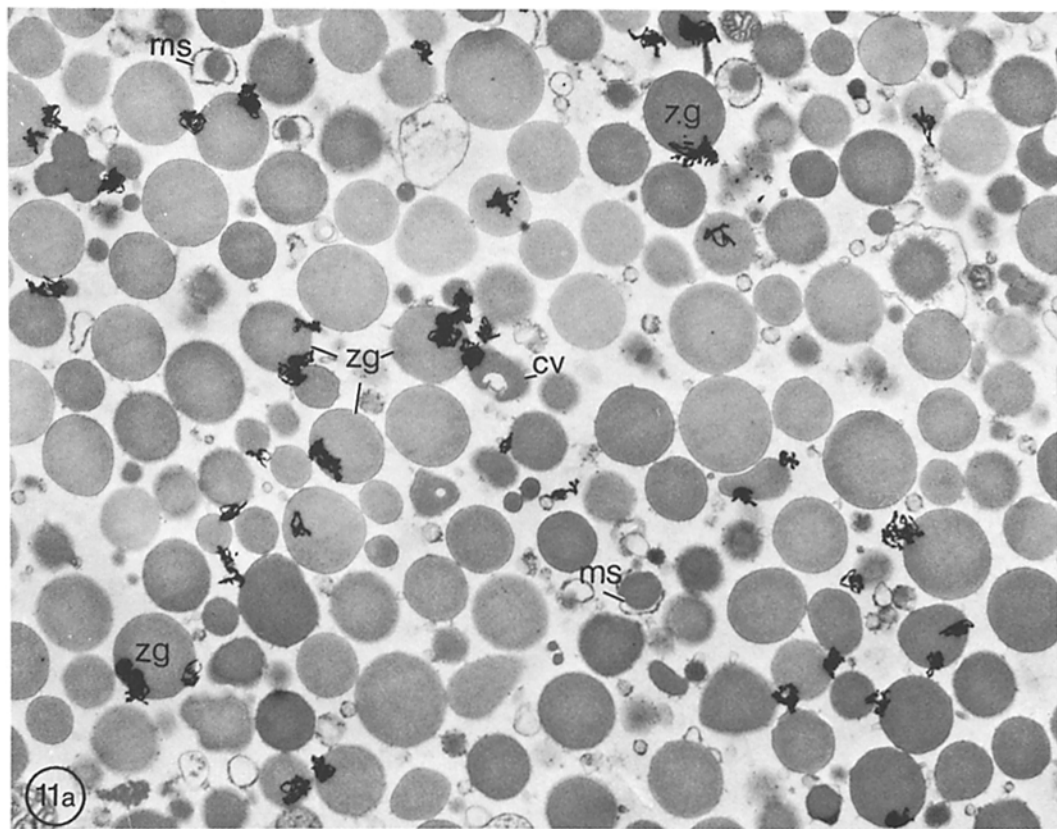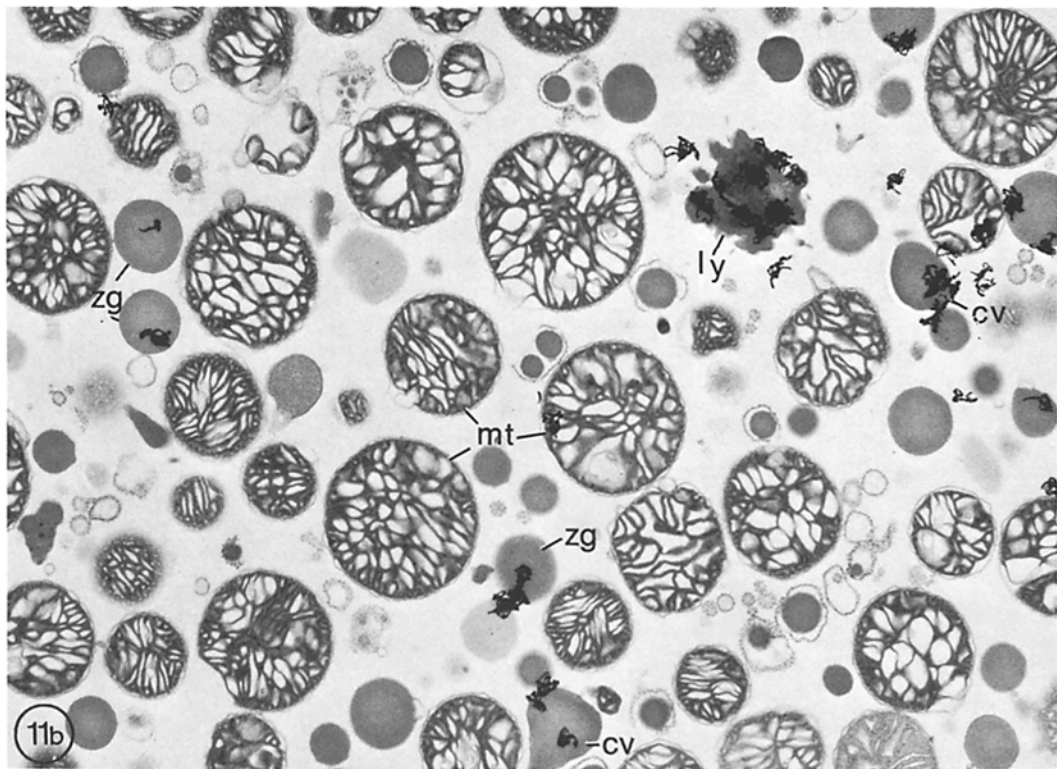
Table V

Fractionation of Pancreatic Lobules Doubly Labeled in Vitro with [³H]Leucine and [³⁵S]Sulfate

Preparation	[³H]Leucine				[³⁵S]Sulfate			
	Counts*	Percent			Counts*	Percent		
Homogenate	21.0 × 10⁶				1.37 × 10⁶			
Nuclear pellet	6.6 × 10⁶				0.48 × 10⁶			
Postnuclear supernate	13.9 × 10⁶	100.0			0.81 × 10⁶	100.0		
Post zymogen supernate		68.0				73.0		
Zymogen granule fraction (crude)		27.8	100.0			20.8	100.0	
Washes			10.3				12.5	
Zymogen granule fraction (washed)			17.5	100.0			8.3	100.0
Content				94.5				61.9
Membranes				5.0				37.2

Minilobules, doubly labeled in vitro with 5 μCi/ml [³H]leucine and 100 μCi/ml $^{35}SO_4^{2-}$ for 60 min, then chased in regular KRB for 45 min, were homogenized and fractionated to obtain a zymogen granule fraction. The latter was lysed in 40 mM NaCl, 125 mM NH₄HCO₃, pH 8.5, and the lysate was centrifuged to sediment the granule membranes. ³H- and ³⁵S-radioactivity were determined in each fraction. Representative experiment in a series of five in which the ³⁵S-radioactivity recovered in the zymogen granule membranes varied from 37 to 50%.

* Total TCA-precipitable counts.

Table VI

Distribution of ³H- and ³⁵S-Radioactivity in Cell Fractions Obtained in a Mixing Experiment

Preparation	TCA-precipitable radioactivity					
	[³H]Leucine			[³⁵S]Sulfate		
	counts*	%		counts*	%	
Homogenate	24.7 × 10⁶			1.15 × 10⁶		
Nuclear pellet	10.8 × 10⁶			0.09 × 10⁶		
Postnuclear supernate	9.0 × 10⁶	100.0		0.95 × 10⁶	100.0	
Post zymogen supernate		72.6			88.8	
Zymogen gr. fraction (crude)		24.9			2.48	
Washes			11.4			1.90
Zymogen gr. fraction (washed)			13.5			0.58

Minilobulues, labeled in vitro for 60 min with [³H]leucine (5 μCi/ml), and chased in regular KRB for 45 min, were homogenized in the final supernate of a similar preparation labeled for 60 min with $^{35}SO_4^{2-}$ (1 mCi/ml). Cell fractions were obtained and counted for ³⁵S- and ³H-radioactivity as given under Materials and Methods, sections *f* and *e*. Representative experiment in a series of four. In the three other experiments, the ³⁵S-radioactivity recovered in the zymogen granule fraction was close to 0.1%.

* Total TCA-precipitable counts.

Figure 11   EM autoradiographs at two different levels in a zymogen granule pellet prepared from minilobules labeled in vitro for 120 min with $^{35}SO_4^{2-}$ (1 mCi/ml), and then chased for 45 min in regular KRB. (*a*) Representative field in the bottom half of the pellet. Most of the autoradiographic grains are associated with zymogen granules (*zg*) and condensing vacuoles (*cv*). Most of the recognizable contaminants, primarily microsomes containing intracisternal granules (*ms*), are not labeled. × 8,000. (*b*) Representative field in the upper quarter of the pellet. Most of the particulate components found at this level are mitochondria (*mt*), but most of the autoradiographic grains are associated with condensing vacuoles (*cv*) and zymogen granules (*zg*). The few lysosomes, e.g. (*ly*), which contaminate this layer are heavily labeled. × 10,000.

compounds in the zymogen granules of the pancreatic exocrine cells of the guinea pig. Since possible sources of particulate or molecular contamination can be ruled out at this level, we decided to use zymogen granule fractions as the starting material for the isolation of extractable sulfated compounds.

SDS-GEL ELECTROPHORESIS: Attempts to isolate them by electrophoresis in SDS-gels (see Materials and Methods, section k) were unsuccessful. The electrophoretograms of zymogen granule extracts on gradient (5-15%) polyacrylamide gels showed the usual pattern of secretory proteins (cf. reference 41) by either Coomassie Blue staining or distribution of ^{3}H-radioactivity (when the lobules had been labeled in vitro with [^{3}H]leucine), but ^{35}S-radioactivity was found smeared throughout the gels with only a few minor peaks (Fig. 12). The electrophoretic mobility of the sulfated compounds could be affected by their sulfate or carbohydrate content (cf. refer-

ences 43 and 47), and especially by aggregation prior to electrophoresis. This would explain the concentration of ^{35}S-radioactivity on top of the gels, but not the smear of radioactivity in the running gels, a finding for which we do not have at present a satisfactory explanation, but which suggests the presence of sulfated compounds of low molecular weight in the zymogen granule extract.

GEL FILTRATION ON SEPHADEX G 150: In our next attempts, extracts of zymogen granule fractions isolated from doubly labeled ([^{3}H]leucine and ^{35}SO$_4^{2-}$) minilobules were fractionated on Sephadex G 150 columns (Fig. 13a), as given under Materials and Methods (section l). The secretory proteins, labeled with [^{3}H]leucine, were resolved into two major peaks. A third peak, which eluted at 3 V_0, probably represented free [^{3}H]leucine or labeled amylase. The latter is known to be retarded on Sephadex gels by affinity interactions (47).
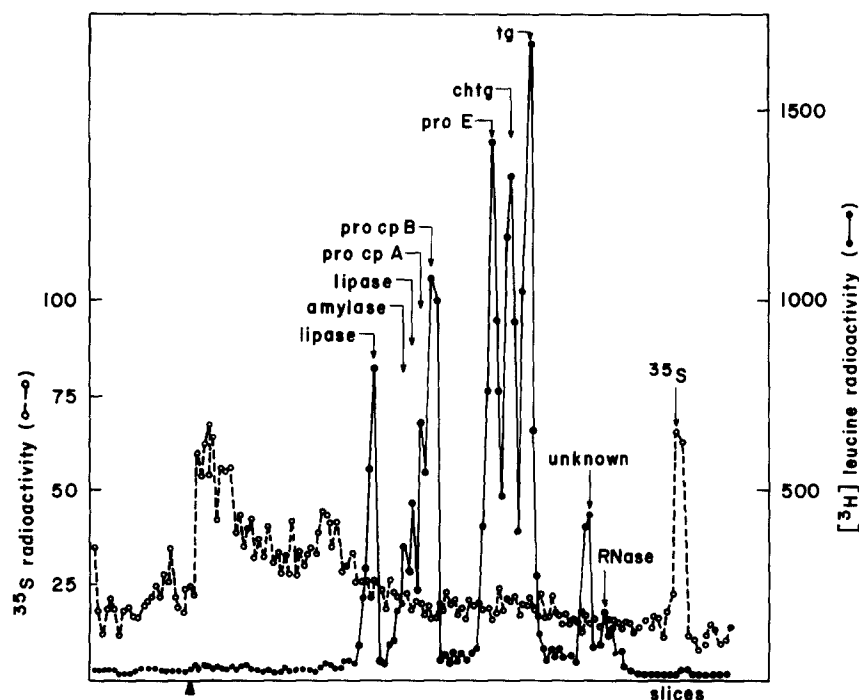

FIGURE 12 Electrophoretogram of a reduced and alkylated zymogen granule extract. The granules were isolated as a zymogen granule fraction from minilobules doubly labeled in vitro with [^{3}H]leucine and ^{35}SO$_4^{2-}$. The gel was processed, sliced, and counted as described under Materials and Methods, section k. The arrow marks the end of the stacking gel. ^{3}H-radioactivity, ●——●; ^{35}S-radioactivity, O- - -O. The secretory proteins of each peak are identified by their full name or by the following abbreviations: pro cp A and pro cp B, procarboxypeptidase A and B; pro E, proelastase; chtg, chymotrypsinogen; tg, trypsinogen; RNase, ribonuclease.

^{35}S-radioactivity was resolved into two major peaks: a high molecular weight fraction which eluted with the void volume (V_0) was well separated from the bulk of secretory proteins, and contained only a small amount of ^{3}H-radioactivity; and a low molecular weight peak which eluted at 3 V_0.

Since sulfated low molecular weight compounds were detected on SDS-gel electrophoretograms, this second peak was pooled, lyophilized, redissolved in 50 mM NH$_4$HCO$_3$, and rechromatographed on Sephadex G 10 columns in the same buffer, or on Sephadex G 25 superfine columns (0.9 × 180 cm) in 10% propionic acid. The ^{35}S-label eluted at exactly the same volume as free ^{35}SO$_4^{2-}$ in both systems; accordingly, we concluded that it represented either free sulfate or small (<700 mol wt) sulfated molecules. These molecules were not sulfated lipids, since <1% of the ^{35}S-radioactivity could be extracted by a chloroform-methanol mixture (cf. reference 15). At present we do not know whether small, sulfated molecules are a regular component of the zymogen granules or an adsorbed contaminant. The second alternative cannot be ruled out on the basis of our mixing experiments since in that case small molecules were expected to be removed by TCA precipitation. Since they could be, however, degradation products of the macromolecular components in the first ^{35}S-radioactivity peak, the latter was also pooled, lyophilized, and redissolved in 0.25 M Tris-HCl buffer, pH 8, containing 0.3 M Na acetate, 0.25 M NaCl, and 50 mg/ml BSA. When this solution was rechromatographed on the same Sephadex G 150 column, the high molecular weight sulfated compounds eluted as before with the void volume without generating breakdown products of smaller molecular weight.

Extracts of doubly labeled zymogen granules were also chromatographed on the same column (Sephadex G 150) in high salt (100 mM NH$_4$HCO$_3$-500 mM NaCl) to test the possibility that the high molecular weight peak might be formed by ionic aggregates of smaller macromolecules. The results showed that, under these conditions, the peak was slightly broadened, but that its elution volume and the amount of radioactivity associated with it remained unchanged (Fig. 13b). In high salt, the [^{3}H]leucine label gave a single, broad peak for secretory proteins and a reduced third peak, suggesting that weak ionic interactions between the Sephadex gel and the secretory proteins affected the distribution of
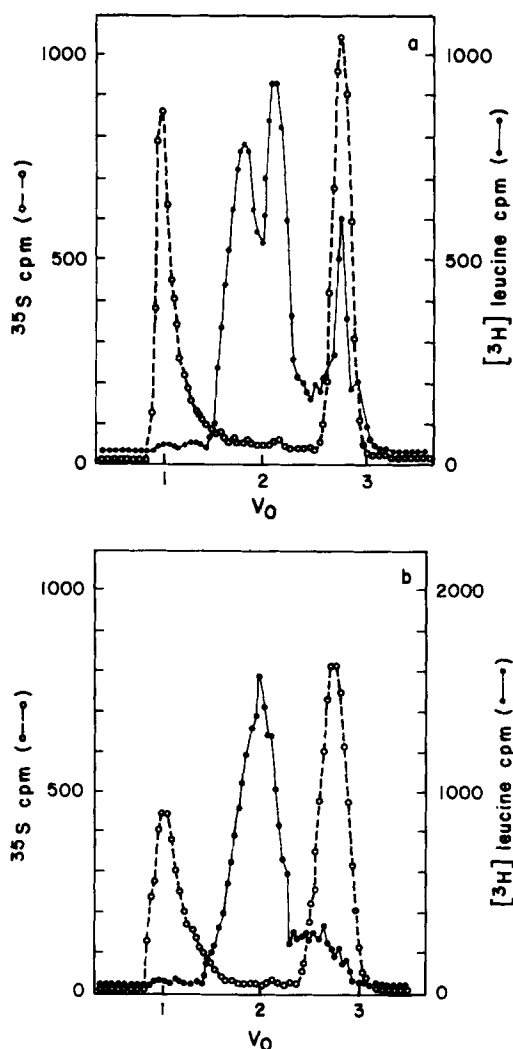

FIGURE 13 Gel filtration on a Sephadex G 150 column of the extract of a zymogen granule fraction isolated from minilobules labeled in vitro with [^{3}H]leucine and ^{35}SO$_4^{2-}$. The column was equilibrated and developed with 100 mM NH$_4$HCO$_3$ in Fig. 13a, or with 100 mM NH$_4$HCO$_3$-500 mM NaCl (high salt) in Fig. 13b. (See Materials and Methods, sections f and g for cell fractionation and zymogen granule extraction, and section l for gel filtration). [^{3}H]leucine radioactivity, ●——●; ^{35}S-radioactivity, O- - -O.

the latter at lower salt concentrations (Fig. 13b).

A small amount of ^{3}H-radioactivity (introduced as [^{3}H]leucine) was found associated with the first ^{35}S-labeled peak under all experimental conditions so far tested. Since we were not able to separate

the two labels, we assume that they are covalently linked in the same molecules.

GEL FILTRATION ON SEPHAROSE 4 B: To assess the molecular weight of the sulfated compounds eluted with the void volume on Sephadex G 150 columns, doubly labeled extracts of zymogen granule fractions were chromatographed on Sepharose 4 B columns as indicated under Materials and Methods, section *l*.

In this case, the sulfated high molecular weight compounds were included in the gel and eluted as a single, nearly symmetrical, but relatively broad peak (Fig. 14) with an estimated average mol wt of 250,000. This figure should be taken as a first approximation, which remains to be checked against additional markers and by other procedures. The shape and breadth of the peak suggested that the high molecular weight sulfated compounds have a heterogeneous size distribution. A second ^{35}S-radioactivity peak, which eluted at 3 V$_0$, is probably free sulfate (cf. gel filtration on Sephadex G 150). The separation of the first ^{35}S-radioactivity peak from the bulk of secretory proteins was less satisfactory than that
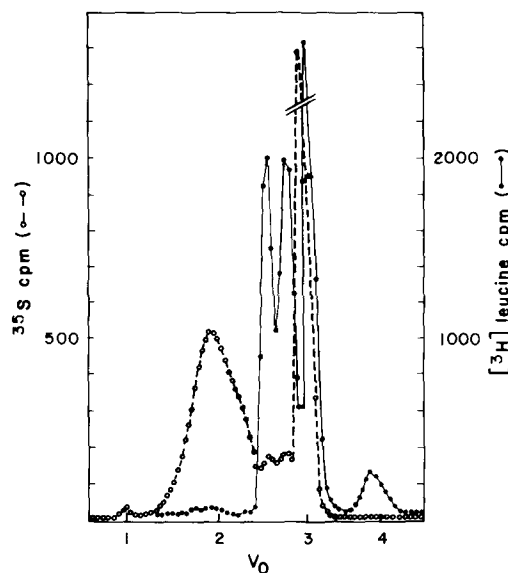

FIGURE 14 Gel filtration on a Sepharose 4B column of the extract of a zymogen granule fraction isolated from minilobules doubly labeled in vitro with [^{3}H]leucine and ^{35}SO$_4{}^{2-}$. The column was equilibrated and developed with 100 mM NH$_4$HCO$_3$, pH 8.3. See Materials and Methods, section *l*, for further details. [^{3}H]leucine radioactivity, ●——●; ^{35}S-radioactivity, O‑ ‑ ‑O.

obtained on Sephadex G 150 columns. A third ^{3}H-radioactivity peak which eluted at 4 V$_0$ might be amylase retarded by affinity interaction with Sepharose 4 B. Rechromatography on Sepharose 4 B of the void volume peak obtained on Sephadex G 150 columns gave an included peak which in position, shape, and recovery was identical to the 250,000 mol wt peak mentioned above.

PARTIAL CHEMICAL CHARACTERIZATION: Preliminary analyses, carried out as given under Materials and Methods, section *m*, showed that the sulfated high molecular weight peak contained amino acids, uronic acids, and amino sugars, namely glucosamine and galactosamine. ^{35}SO$_4{}^{2-}$ liberation upon hydrolysis in 0.04 N HCl, and partial depolymerization by direct treatment with nitrous acid (25) indicated that molecules behaving like heparin or heparan sulfate accounted for ~75% of the ^{35}S-radioactivity of the peak. Treatment of peak samples with chondroitinase ABC (36) resulted in an ~20% loss of ^{35}S-radioactivity; hence, chondroitin sulfate appeared to be a minor component of the sulfated macromolecular peak. The relative proportions of these compounds varied, however, from experiment to experiment, reflecting perhaps, variations in the extent of extraction of sulfated compounds from the membrane pellet. The exact proportions of these compounds and their relations to the nonextractable sulfated fraction of the zymogen granule membranes remain to be established by further investigations.

DISCUSSION

We have already mentioned in the introduction the findings that led to the hypothesis that concentration of secretory proteins in Golgi condensing vacuoles is obtained by the formation of aggregates primarily by ionic interactions between secretory proteins and sulfated polyanions. Such aggregates may be less hydrophilic than their component molecules; in addition, their formation may lead to a progressive reduction of osmotic activity within condensing vacuoles with water outflow as the immediate consequence. The proposed mechanism is potentially of broad significance, since concentration of secretory proteins is a mandatory step in the formation of secretion granules, which (in turn) is a prerequisite for intracellular storage and regulated discharge in a variety of glandular cells. In the exocrine pancreatic cell of the guinea pig, ionic interactions are

expected to play an important role, given the prevailing cationic nature of the secretory proteins and the low pI of the sulfated compounds, but in other glandular cells other types of interactions (stereospecific, formation of metal-protein complexes) may lead to the same result (cf. reference 22). To operate efficiently, a concentrating system of this type requires that one of the interacting species (e.g. the sulfated polyanion) be generated (or become functional) only at the site of concentration, i.e., the Golgi complex. In fact, the autoradiographic studies so far published indicate that the primary site of $^{35}SO_4^{2-}$ incorporation is the Golgi complex (cf. reference 50).

The dual goal of the present study was to extend to the pancreatic acinar cell of the guinea pig the detection and identification of sulfation sites by autoradiography, and to isolate the sulfated polyanions from an adequate source, as a prerequisite for its chemical characterization. In our attempts to achieve these goals, we have encountered a number of problems which had to be recognized and solved (when possible) before proceeding further.

Multiple Sites of Sulfation

The first problem stemmed from the discovery (by autoradiography) that $^{35}SO_4^{2-}$ is actively incorporated by the epithelium of the entire duct system of the gland. In centroacinar cells and epithelia of intralobular ducts, the rate of $^{35}SO_4^{2-}$ incorporation is comparable to that found in acinar cells; but in the epithelial cells of interlobular ducts and especially in those of the main collecting duct (and its immediate affluents) the rate is considerably higher. Recognizable goblet cells are found only in the last two locations, and their rate of discharge appears to be slow, as seems to be the case with goblet cells in other epithelia (27, 30, 31), yet their products are expected to appear in secretion collected by cannulation of the main duct. Of considerable interest is the active incorporation of $^{35}SO_4^{2-}$ by the cells of the regular duct epithelium. In these cells, the label is initially found over the Golgi complex and the plasmalemma, especially over the latter's luminal domain, but later on autoradiographic grains also appear over the luminal content. The nature of the sulfated compounds synthesized by the ductal epithelium is entirely unknown; their preferential association with the plasmalemma suggests that at least some of these compounds are sulfated glycolipids, as in the case of the nephron epithelium

(15), but others could be sulfated glycoproteins, as in the intestinal epithelium (19). Our observations do not establish that the epithelial cells of the ducts secrete sulfated compounds into the glandular lumina, nor do they rule out the possibility that such products are shed or discharged into the pancreatic juice. Since the pancreatic ducts, including their intralobular segments, represent a potential source of sulfated compounds, we could not use the secretion collected from lobules labeled in vitro with $^{35}SO_4^{2-}$ as a starting preparation for the sulfated compounds of interest.

Sulfated Compounds in Acinar Cells

In acinar cells, our autoradiographic experiments have established the presence of newly synthesized sulfated compounds in all distal secretory structures, i.e., in Golgi vesicles, stacks of Golgi cisternae, condensing vacuoles, and zymogen granules. In addition, the autoradiography of isolated zymogen granule fractions confirmed the presence of sulfated compounds in condensing vacuoles and secretion granules and showed that these fractions (especially after removing their top layers) are essentially free of ^{35}S-labeled, particulate contaminants.

The results of our mixing experiments strongly suggest that the association of sulfated compounds with zymogen granules does not reflect the relocation by adsorption of ^{35}S-labeled molecules liberated from other intra- or extracellular compartments upon tissue homogenization. Admittedly, these experiments do not provide definitive proof for the absence of this type of molecular contamination, since we have not established that adsorbed sulfated compounds can be actually removed from zymogen granules under our experimental conditions. Our conclusion is supported, however, by recent results which indicate that relocation by adsorption of secretory proteins on zymogen granules is limited or negligible (46), especially in the case of anionic proteins.[2] From the preceding it appears therefore, that we have established, with a reasonable degree of certitude, the presence of sulfated macromolecular components in zymogen granules and the suitability of zymogen granule fractions as a starting preparation for the isolation and characterization of these compounds.

In the process, however, we have found that ^{35}S-radioactivity derived from $^{35}SO_4^{2-}$ appears not only in distal secretory structures, but also in other

subcellular components, presumably the cytoplasmic matrix or the RER. Our own results (Figs. 12-14), and those already obtained by Tartakoff et al. (44) by isoelectric focusing indicate convincingly that this label is not incorporated into secretory proteins (via cysteine or methionine). With a better correction for radioactivity spread, the actual amount of sulfated components in subcellular compartments other than those of the distal secretory structures may turn out to be modest, yet we found ^{35}S-autoradiographic grains over bona fide rough microsomes in microsomal fractions. At present, the chemical nature of these RER-associated sulfated compounds and their relationship (if any) to the compounds found in distal secretory structures are totally unknown.

Persistence of ^{35}S-Radioactivity in the Golgi Complex

Our autoradiographic data indicate that ^{35}S-radioactivity continues to mark Golgi elements, primarily condensing vacuoles, even after chase periods as long as 3 h, i.e., long after the wave of concurrently labeled secretory proteins would have passed under normal conditions through the Golgi complex. It is conceivable that the persistence of the label reflects a general slowdown in intracellular transport and concentration of secretory products, presumably caused by the long exposure (60 min) of the cells to the low sulfate medium used in our experimental protocol. But the morphology of the cells, especially the appearance of their condensing vacuoles is unaltered, which would suggest that in our case the concentration step is not impaired. A slowdown in transport and concentration has been observed in isolated pancreatic acinar cells by Amsterdam and Jamieson (2); in their case, the condensing vacuoles were visibly affected (1) and the defect in concentration seemed to be connected with the temporary removal of Ca^{2+} which is part of the dissociation procedure. Ca^{2+} is present in detectable amounts in zymogen granules and their membranes (13), and could be one of the interacting species in aggregate formation. At present, two possible explanations could be advanced for the persistence of ^{35}S-label in the Golgi complex: (a) the chase of labeled intermediates in SO_4^{2-} metabolism is not sufficiently effective, and (b) the labeled compounds are interacting with the secretion granule membranes strongly enough to be incompletely discharged upon exocytosis, hence,

partially retrieved upon membrane recovery. The second alternative is supported by the results of our extraction experiments which indicate that the sulfated compounds are less easily extracted than secretory proteins upon the lysis of zymogen granules in alkaline buffer. If this second alternative were to obtain, the sulfated compounds could be used as a natural tag for tracing the intracellular fate of the membranes recovered from the luminal front of the cell after exocytosis.

Preliminary results obtained with pancreatic lobules stimulated to discharge in vitro after double labeling with [^{3}H]leucine and ^{35}SO$_4^{2-}$, suggest that the sulfated polyanions and the secretory proteins of the zymogen granules are not discharged in parallel, the former being extensively retained within the lobules. These results are in keeping with the retention of the sulfated compounds by recoverable or recovered membranes at the level of the acinar cells, but other explanations (e.g. discharge followed by retention in the acinar lumina) are not excluded.

It should be mentioned that sulfated macromolecules have recently been detected in parotid acinar cells by autoradiography (7), and in the pancreatic secretion of the mouse by biochemical assays (6). For some time already, sulfated glycosaminoglycans have been used in model experiments to inhibit the activity of lysosomal hydrolases (cf. reference 5). Finally, "soluble acidic lipoproteins" have been assumed to play a role in the formation of storage granules and in the latency of lysosomal enzymes (24), but they appear to be poorly defined mixtures of secretory proteins and membrane components. Hence, it is unlikely that they have anything in common with the sulfated macromolecules we have investigated.

For the moment (and leaving aside all the side issues we have uncovered), our results indicate that sulfated polyanions, presumably sulfated glycosaminoglycans, can be prepared from extracts of zymogen granule fractions by gel filtration on either Sephadex G 150 or Sepharose 4 B. The sulfated compounds can be obtained as a distinct fraction reasonably well separated from the bulk of secretory proteins. With this point established, it is now possible to proceed with their chemical characterization (beyond the preliminary level thus far achieved), and eventually with in vitro tests of their interactions with secretory proteins.

autoradiographic studies; Hans Stukenbrok, for process-
ing the specimens and collecting the electron micro-
graphs for the second set of autoradiographic experi-
ments; Joanne Reid, for quantitating the results of the
second set of experiments; and especially Dr. J. D.
Jamieson, for useful advice in the preparation of mini-
lobules and for sustained interest during the entire
project.

REFERENCES

1. Amsterdam, A., and J. D. Jamieson. 1974. Stud-
   ies on dispersed pancreatic exocrine cells. I. Disso-
   ciation technique and morphologic characteristics of
   separated cells. *J. Cell Biol.* **63:**1037-1056.
2. Amsterdam, A., and J. D. Jamieson. 1974. Stud-
   ies on dispersed pancreatic exocrine cells. II. Func-
   tional characteristics of separated cells. *J. Cell Biol.*
   63:1057-1073.
3. Amsterdam, A., T. E. Solomon, and J. D. Jamie-
   son. 1977. Sequential dissociation of the exocrine
   pancreas into lobules, acini, and individual cells. *In*
   Methods in Cell Biology. Vol. 19. D. M. Prescott,
   editor. Academic Press, Inc., New York. In press.
4. Anderson, L. E., and W. O. McClure. 1973. An
   improved scintillation cocktail of high-solubilizing
   power. *Anal. Biochem.* **51:**173-179.
5. Avila, J. L., and J. Convit. 1976. Physicochemi-
   cal characteristics of the glycosaminoglycan-lysoso-
   mal enzyme interaction *in vitro*. A model of control
   of leukocytic lysosomal activity. *Biochem. J.*
   160:129-136.
6. Berg, N. B. 1976. Sulfated macromolecules in the
   exocrine pancreas. *Anat. Rec.* **184:**358-359.
7. Berg, N. B., and B. P. Austin. 1976. Intracellular
   transport of sulfated macromolecules in parotid
   acinar cells. *Cell Tissue Res.* **165:**215-255.
8. Berg, N. B., and R. W. Young. 1971. Sulfate
   metabolism in pancreatic acinar cells. *J. Cell Biol.*
   50:469-483.
9. Bitter, T., and H. M. Muir. 1962. A modified
   uronic acid carbazole reaction. *Anal. Biochem.*
   4:330-334.
10. Bolender, R. T. 1974. Stereological analysis of
    the guinea pig pancreas. I. Analytical model and
    quantitative description of nonstimulated pancreatic
    exocrine cells. *J. Cell Biol.* **61:**269-287.
11. Burton, K. 1956. A study of the conditions and
    mechanism of the diphenylamine reaction for the
    colorimetric estimation of desoxyribonucleic acid.

Biochem. J. **62:**315-323.
12. Caro, L., and R. P. Van Tubergen. 1962. High
    resolution autoradiography. I. Methods. *J. Cell
    Biol.* **15:**173-188.
13. Clementi, F., and J. Meldolesi. 1975. Calcium
    and pancreatic secretion. I. Subcellular distribution
    of calcium and magnesium in the exocrine pancreas
    of the guinea pig. *J. Cell Biol.* **65:**88-102.
14. Eagle, E. 1959. Amino acid metabolism in mam-
    malian cell cultures. *Science (Wash. D. C.).*
    130:432-437.
15. Fleischer, B., and F. Zambrano. 1974. Golgi
    apparatus of rat kidney. Preparation and role in
    sulfatide formation. *J. Biol. Chem.* **249:**5995-6003.
16. Giannattasio, G., and A. Zanini. 1976. Pres-
    ence of sulfated proteoglycans in prolactine secre-
    tory granules isolated from the rat pituitary gland.
    Biochim. Biophys. Acta. **439:**349-357.
17. Glossmann, H., and D. M. Neville. 1971. Gly-
    coproteins of cell surfaces. *J. Biol. Chem.*
    246:6339-6346.
18. Godman, G. C., and N. Lane. 1964. On the site
    of sulfatation in the chondrocyte. *J. Cell Biol.*
    21:353-366.
19. Ito, S. 1965. Radioactive labelling of the surface
    coat on enteric microvilli. *Anat. Rec.* **151:**489
    (Abstr.).
20. Jamieson, J. D., and G. E. Palade. 1967. Intra-
    cellular transport of secretory proteins in the pan-
    creatic exocrine cell. Transport to condensing vacu-
    oles and zymogen granules. *J. Cell Biol.* **34:**597-
    615.
21. Jamieson, J. D., and G. E. Palade. 1971. Con-
    densing vacuole conversion and zymogen granule
    discharge in pancreatic exocrine cells: metabolic
    requirements. *J. Cell Biol.* **48:**503-522.
22. Jamieson, J. D., and G. E. Palade. 1977. Produc-
    tion of secretory proteins in animal cells. *In* Inter-
    national Cell Biology 1976-1977. B. R. Brinkley
    and K. R. Porter, editors. The Rockefeller Univer-
    sity Press. 308-317.
23. Katona, E. 1976. Incorporation of inorganic sul-
    fate in rat-liver Golgi. *Eur. J. Biochem.* **63:**583-
    590.
24. Koenig, H. 1974. The soluble acidic lipoproteins
    (SALPS) of storage granules. Matrix constituents
    which may bind stored molecules. *Adv. Cytophar-
    macol.* **2:**273-301.
25. Kraemer, P. M. 1971. Heparan sulfates of cul-
    tured cells. I. Membrane-associated and cell-sap
    species in Chinese hamster cells. *Biochemistry.*
    10:1437-1445.
26. Lagunoff, D. M., T. Philipps, O. A. Iseri, and
    E. P. Benedit. 1964. Isolation and preliminary
    characterization of rat mast cell granules. *Lab.
    Invest.* **13:**1331-1344.
27. Lane, N., L. Caro, L. R. Otero-Vilardebo, and
    G. C. Godman. 1964. On the site of sulfation in

colonic goblet cells. *J. Cell Biol.* **21**:339–351.

28. MELDOLESI, J., J. D. JAMIESON, and G. E. PALADE. 1971. Composition of cellular membranes in the pancreas of the guinea pig. *J. Cell Biol.* **49**:109–129.

29. NEMOTO, T., and Z. YOSIZAWA. 1969. Sulfated glycopeptides and glycoaminoglycan peptides isolated from intestinal mucosa of rabbit. *Biochim. Biophys. Acta.* **192**:37–48.

30. NEUTRA, M., and C. P. LEBLOND. 1966 a. Synthesis of the carbohydrate of mucus in the Golgi complex as shown by electron microscope radioautography of goblet cells from rats injected with glucose-^{3}H. *J. Cell Biol.* **30**:119–136.

31. NEUTRA, M., and C. P. LEBLOND. 1966. Radioautographic comparison of the uptake of galactose-^{3}H and glucose-^{3}H in the Golgi region of various cells secreting glycoproteins or mucopolysaccharides. *J. Cell Biol.* **30**:137–150.

32. NEVILLE, D. M. 1971. Molecular weight determination of protein-dodecylsulfate complexes by gel electrophoresis in a discontinuous buffer system. *J. Biol. Chem.* **246**:6328–6334.

33. OLSSON, L., and S. GARDELL. 1967. Isolation and characterization of glycosaminoglycans from human leukocytes and platelets. *Biochem. Biophys. Acta.* **141**:348–357.

34. REGGIO, H. A., and G. E. PALADE. 1976. Sulfated compounds in the secretion and zymogen granule content of the guinea pig pancreas. *J. Cell Biol.* **70** (2, Pt. 2):360*a*. (Abstr.).

35. RICHARDSON, K. C., L. JARETT, and E. H. FINKE. 1960. Embedding in epoxy resins for ultrathin sectioning in electron microscopy. *Stain Technol.* **35**:313–323.

36. SAITO, H., T. YAMAGATA, and S. SUZUKI. 1968. Enzymatic methods for determination of small quantities of isomeric chondroitin sulfates. *J. Biol. Chem.* **243**:1536–1542.

37. SALPETER, M. M., and L. BACHMANN. 1972. *In* Principles and Techniques in Electron Microscopy. M. A. Hayat, editor. Van Nostrand Reinhold Co., New York. **2**:221–278.

38. SALPETER, M. M., L. BACHMANN, and E. E. SALPETER. 1969. Resolution in electron microscope radioautography. *J. Cell Biol.* **41**:1–20.

39. SALPETER, M. M., and F. C. McHENRY. 1973. Electron microscope autoradiography. Analyses of autoradiograms. *In* Advanced Techniques in Biological Electron Microscopy. J. K. Koehler, editor. Springer-Verlag, New York. 113–152.

40. SALPETER, M. M., and E. E. SALPETER. 1971. Resolution in electron microscope radioautography. II. Carbon^{14}. *J. Cell Biol.* **50**:324–332.

41. SCHEELE, G. A. 1975. Two dimensional gel analysis of soluble proteins. Characterization of guinea pig exocrine pancreatic proteins. *J. Biol. Chem.* **250**:5375–5385.

42. SCHEELE, G. A., and G. E. PALADE. 1975. Studies on the pancreas of the guinea pig. Parallel discharge of exocrine enzyme activities. *J. Biol. Chem.* **250**:2660–2670.

43. SEGREST, J. R., R. L. JACKSON, E. P. ANDREWS, and V. T. MARCHESI. 1971. Human erythrocyte membrane glycoprotein; a re-evaluation of the molecular weight as determined by SDS-polyacrylamide gel electrophoresis. *Biochem. Biophys. Res. Commun.* **44**:390–395.

44. TARTAKOFF, A., L. J. GREENE, and G. E. PALADE. 1975. Studies on the pancreas of the guinea pig. Fractionation and partial characterization of exocrine proteins. *J. Biol. Chem.* **249**:7420–7431.

45. TARTAKOFF, A., and J. D. JAMIESON. 1974. Subcellular fractionation of the pancreas. *Methods Enzymol.* **31**:41–59.

46. TARTAKOFF, A., J. D. JAMIESON, G. A. SCHEELE, and G. E. PALADE. 1975. Studies on the pancreas of the guinea pig. Parallel processing and discharge of secretory proteins. *J. Biol. Chem.* **250**:2671–2677.

47. VANDERMEERS, A., and J. CHRISTOPHE. 1967. Amylase et lipase du pancreas de rat. Purification chromatographique, recherche du poids moleculaire et composition en acides amines. *Biochim. Biophys. Acta.* **154**:110–129.

48. VENABLE, J. H., and R. COGGESHALL. 1965. A simplified lead citrate stain for use in electron microscopy. *J. Cell Biol.* **25**:407–408.

49. WEIBEL, E. R. 1969. Stereological principles for morphometry in electron microscopic cytology. *Int. Rev. Cytol.* **26**:235–302.

50. YOUNG, R. W. 1973. The role of the Golgi complex in sulfate metabolism. *J. Cell Biol.* **57**:175–189.